Supporting Information

Self-Assembly of Tetraphenylethylene-Cored Metallacycles Linked by Stereo-isomerizable Ligands: Photo-induced E to Z isomerization within Supramolecular Structures

Bing-Yu Li, Jin Tong*, Ji Wang, Shu-Yan Yu*

Center of Excellence for Environmental Safety and Biological Effects, State Key Laboratory of Materials Low-Carbon Recycling, College of Chemistry and Life Science, Beijing University of Technology, Beijing 100124, China

* To whom correspondence should be addressed: E-mail: jintong@bjut.edu.cn, selfassembly@bjut.edu.cn

1. Instruments and measurements

All chemicals were purchased from commercial suppliers and all of the solvents were further purified according to conventional methods. The water used in the experiment was purified by the laboratory water purification system of BEST series. ^{1}H NMR, ^{13}C NMR, ^{1}H-^{1}H NOESY, ^{1}H-^{1}H COSY spectra of all compounds were carried out on a Bruker 400 MHz spectrometer in DMSO-d_6 solution with TMS as internal standard at room temperature. Mass spectra were recorded on a JEOL Accu-TOF-4G LC-plus mass spectrometer. The UH-4150 UV/Vis spectrophotometer was utilized to get absorption spectra. Column chromatography was performed on silica gel (200–300 mesh).

2. Synthetic details of H_2Z and H_2E

Trans- and cis-isomers of H_2Z and H_2E were synthesized as shown in Scheme S1.

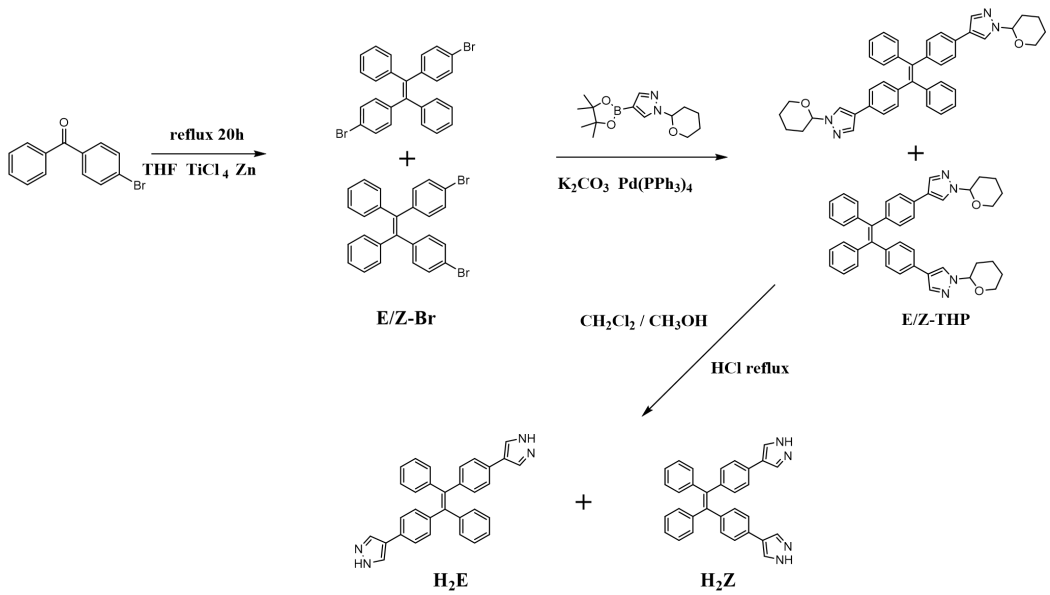

Scheme S1. Synthetic route to the synthesis of H_2E and H_2Z.

The configuration-controllable precursors Z-P and E-P of the H_2E / H_2Z isomers are first provided using a Pd-catalyzed Suzuki-Miyaura coupling reaction. Detailed synthetic processes and structural characterizations are provided in the Experimental Section. It is important to note that both the trans- and cis-isomers of the ligands display poor solubility in organic solvents, which results in difficulties in separating via column chromatography. In contrast, the two isomers

of precursors, Z-P and E-P, show different Rf values on TLC using dichloromethane and ethyl acetate (5:1, v/v) as eluent due to their structural differences. The two isomers were successfully separated through careful column chromatography, and their structures were confirmed by nuclear magnetic resonance (NMR) spectroscopy.

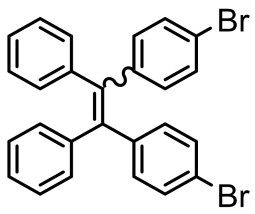

Synthesis of 1,2-Bis(4-bromophenyl)-1,2-diphenylethene (Z/E-Br)

4-Bromobenzophenone (2 g, 7.66 mmol) and zinc powder (1.5g ,23.08 mmol) were placed in a three-necked flask (250 mL) under an nitrogen atmosphere at -78℃. Then dry THF (100 mL) was placed in the flask through the branch. Then titanium tetrachloride (5 mL, 45.63 mmol) was added with rapid stirring over approximately 30 min. The mixture was refluxed for 20 h at 90 °C. Then, the product was filtered and then vacuum-evaporated then extracted three times with dichloromethane. After it was washed with water and dried with Mg_2SO_4. The final products were purified by column chromatography with pure n-hexane mobile phase final a white powder was gained and Direct used for the next reaction.

Synthesis of 1,2-diphenyl-1,2-bis(4-(1-(tetrahydro-2H-pyran-2-yl)-1H-pyrazol-4-yl)phenyl) ethene (Z-P and E-P).

The preparation of the ligands Z-P and E-P was synthesis by suzuki coupling. The Z/E-Br mixture (2 mmol, 0.96 g), 1-THP-pyrazole borate (4 equiv, 1-(tetrahydro-2H-pyran-2-yl)-4-(4,4,5,5-tetramethyl-1,3,2-dioxaborolan-2-yl)-1H-pyrazole (8 mmol, 2.22 g)), tetrakis(triphenyl-phosphine)palladium ($Pd(PPh_3)_4$; 0.3 mmol, 0.346 g), and potassium carbonate (13.82 mmol, 1.91 g) were placed in

the 250 mL flask. A 90 mL portion of N-butylalcohol and 30mL of water were then also added, and the solution was refluxed at 120 °C for 48 h. The product was first vacuum-evaporated and then extracted three times with dichloromethane. After it was washed with water and dried with anhydrous Mg_2SO_4. The products of *Z*-P and *E*-P were purified by column chromatography with CH_2Cl_2/EA 10/1 and 5/1 mobile phase.

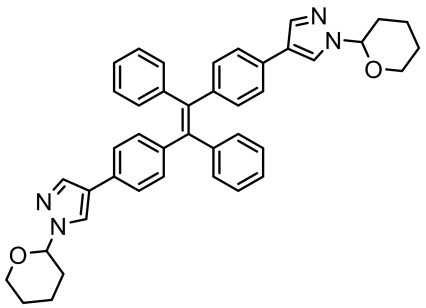

Z-P: Yield 420 mg (33.22%). White powder. ^{1}H NMR (400 MHz, DMSO-d_6, 298K): δ (ppm) 8.27 (s, 2 H), 7.87 (s,2H), 7.39-7.41 (d, 4H, J = 8.34 Hz), 7.10-7.15(m, 6H), 6.99-7.00 (d, 4 H), 6.95-6.97 (d, 4 H), 5.34-5.37 (q, 2 H), 3.58-3.95 (q, 4 H). ^{13}C NMR (100 MHz, DMSO-d_6, 298 K): δ (ppm) 143.7762, 141.6177, 140.5934, 136.7704, 131.6856, 131.2477, 130.9699, 128.2747, 126.9889, 126.2145, 124.9752, 122.3566, 87.3383, 67.2422, 30.2567, 25.0716, 22.4056.

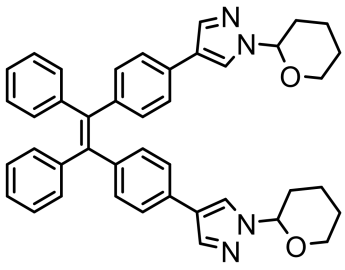

E-P: Yield 510mg (40.34%). White powder. ^{1}H NMR (400 MHz, $CDCl_3$, 298 K): δ (ppm) 7.75-7.78 (d, 4 H, J = 12.20 Hz), 7.21-7.23 (d,4 H, J = 8.16 Hz), 7.06-7.12 (m, 10H), 6.98-7.00 (d, 4H, J = 8.20 Hz), 5.36-5.38 (q, 2 H), 3.69-4.04 (q, 4 H). ^{13}C NMR (100 MHz, DMSO-d_6, 298 K): δ (ppm) 143.7777, 142.0307, 140.5436, 137.0900, 131.8736, 131.4214, 130.4280,127.7808 ,126.4897, 124.7412, 124.3801, 123.2048, 87.7459, 67.7381, 30.5471, 24.9813, 22.3677.

Synthesis of 1,2-Bis(4-(pyrazole-2-yl)phenyl)ethane (H_2Z and H_2E).

The Z-P and E-P protected product was dissolved in dichloromethane and methanol respectively and 1mL hydrochloric acid was added into the solution then reflux 2h. The solution adjusted to pH 7.0 with a saturated aqueous solution of sodium bicarbonate, filtered, washed with a small amount of dichloromethane, and dried to obtain the product (**H_2Z** and **H_2E**)

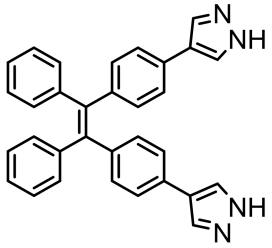

H_2Z: Yield 280mg (30.43%). White powder. ^{1}H NMR (400 MHz, DMSO-d_6, 298K): δ (ppm) 12.90 (s, 2H), 7.99 (s, 4H), 7.39-7.41 (d, 4H, J = 8.28 Hz), 7.12-7.15(t, 4H), 7.08-7.12 (t, 2H), 6.97-6.99 (d, 4H), 6.95-6.97 (d, 4H). ^{13}C NMR (100 MHz, DMSO-d_6, 298 K): δ (ppm) 143.8741, 141.3156, 140.5293, 131.6536, 131.5593, 131.2612, 128.2524, 126.9441, 124.9812, 121.2199. ESI-MS (m/z): $[H_2Z+H]^+$ calculated for $C_{32}H_{25}N_4$: 465.5718; found: 465.2081.

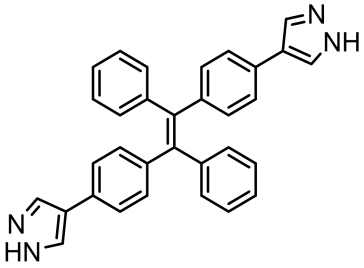

H_2E: Yield 355mg (38.58%). White powder. ^{1}H NMR (400 MHz, DMSO-d_6, 298 K): δ (ppm) 12.90 (s, 2 H), 7.99 (s,4 H), 7.35-7.37 (d, 4H, J = 8.28 Hz), 7.15-7.18(t, 4H), 7.12-7.14 (t, 2H), 7.03-7.15(d, 4H), 6.89-6.92 (d, 4H, J = 8.29 Hz). ^{13}C NMR (100 MHz, DMSO-d_6, 298 K):δ (ppm) 143.9401, 141.2563, 140.5298, 131.6577, 131.4751, 131.2484, 128.3661, 127.0484, 124.8772,

121.2123. ESI-MS (m/z): $[H_2Z+H]^+$ calculated for $C_{32}H_{25}N_4$: 465.5718; found: 465.2061.

3. ^{1}H NMR, ^{13}C NMR, ^{1}H-^{1}H COSY ^{1}H-^{1}H NOESY and FT-MS spectra

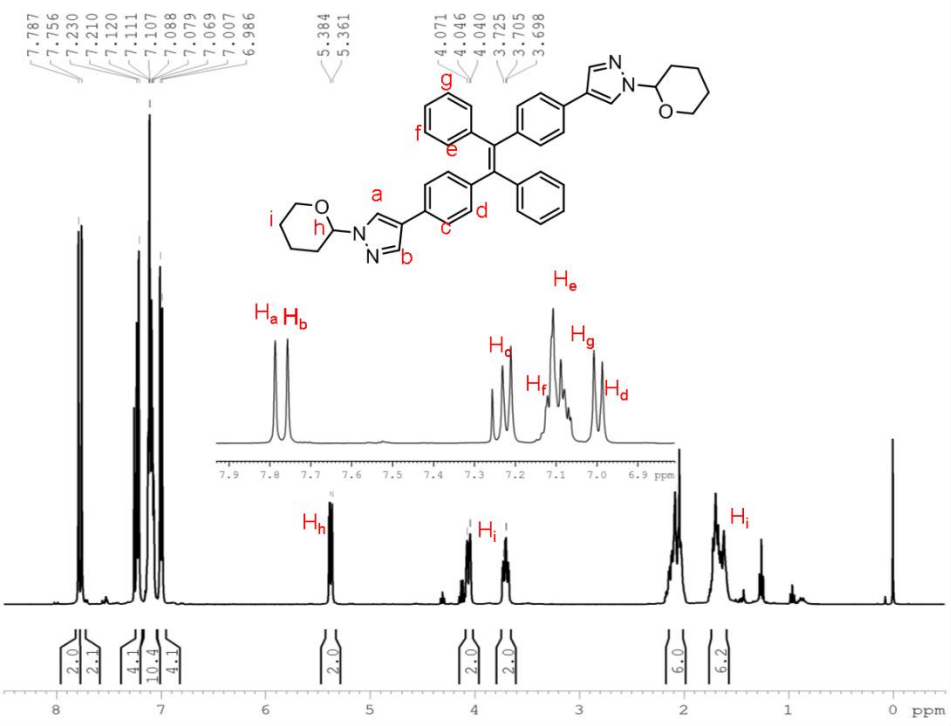

Fig. S1. ^{1}H NMR spectrum of **E-P** (400 MHz, 298K, DMSO-d_6).

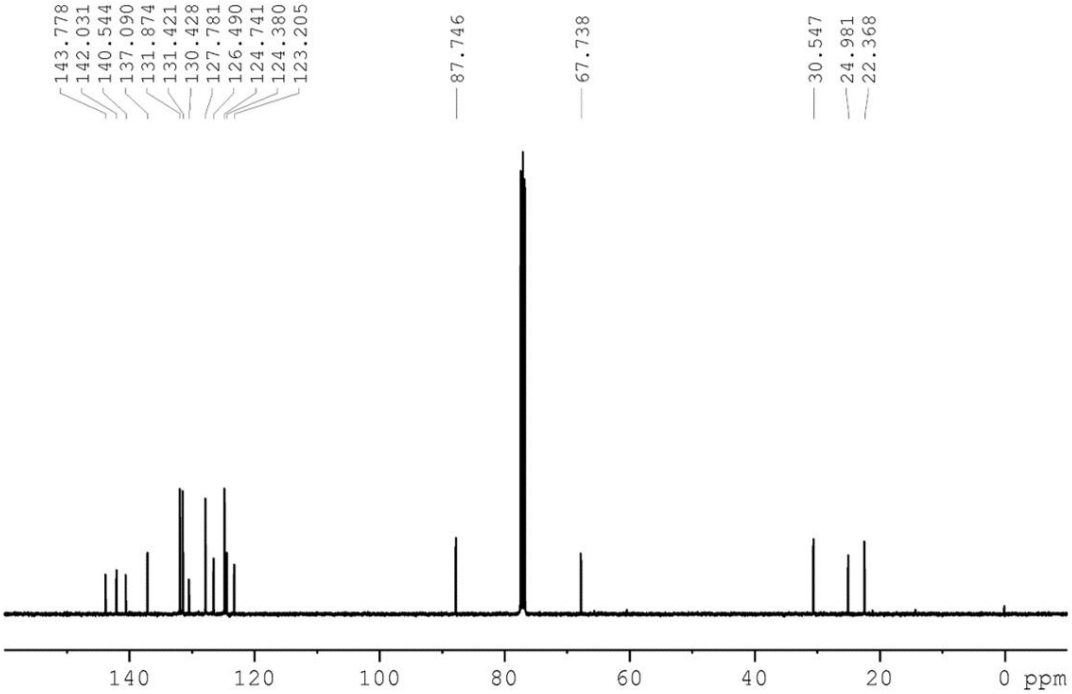

Fig. S2. ^{1}H NMR spectrum of **E-P** (400 MHz, 298 K, DMSO-d_6).

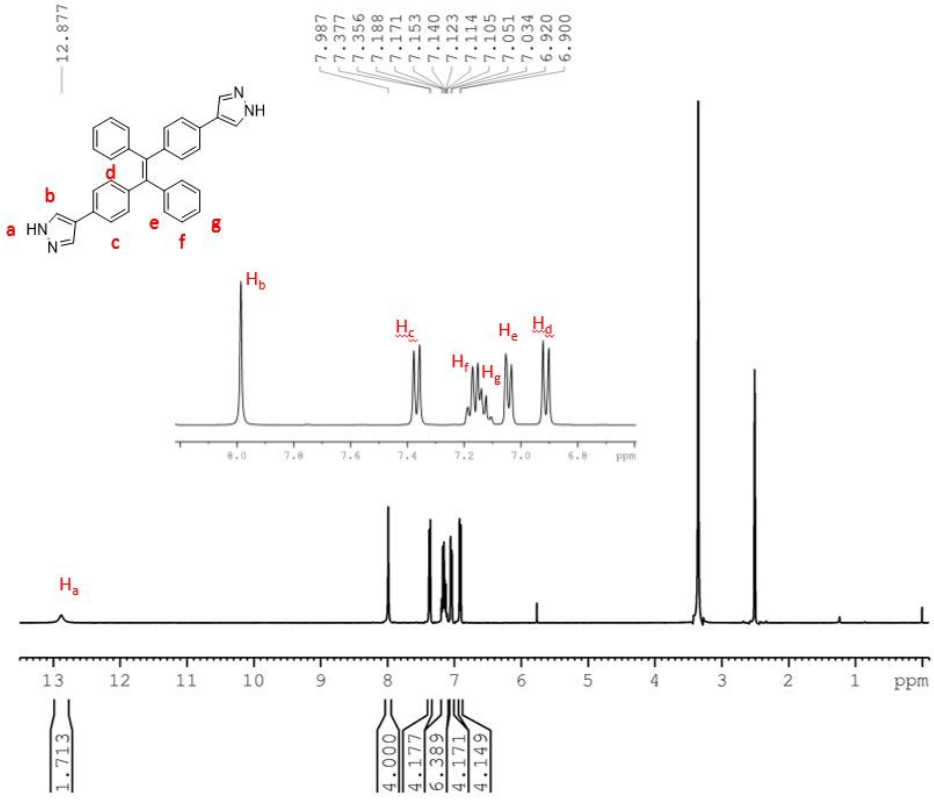

Fig. S3. ^{1}H NMR spectrum of **H_2E** (400 MHz, 298 K, DMSO-d_6).

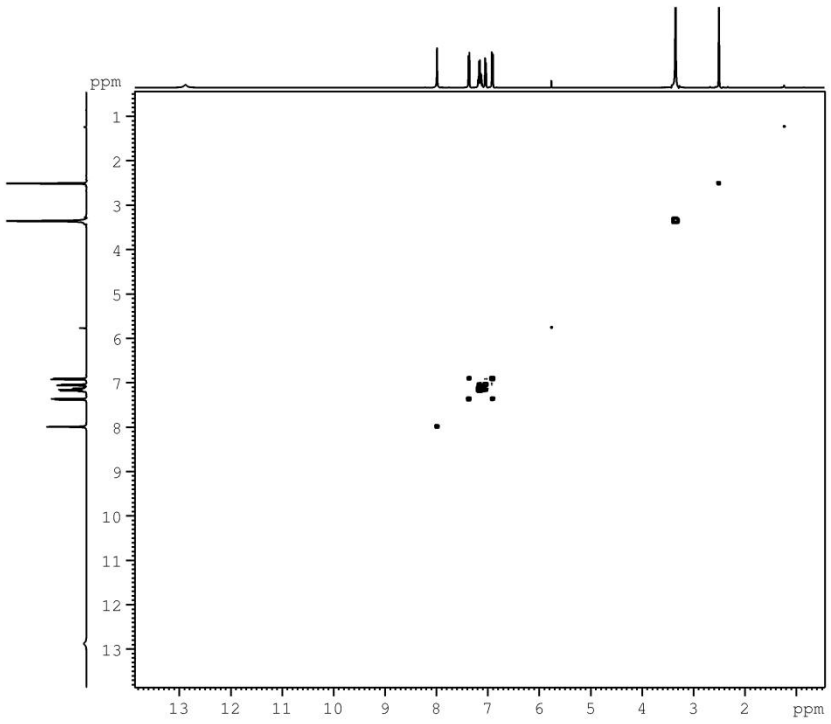

Fig. S4. Full ^{1}H-^{1}H COSY spectrum of **H_2E** (400 MHz, 298 K, DMSO-d_6)

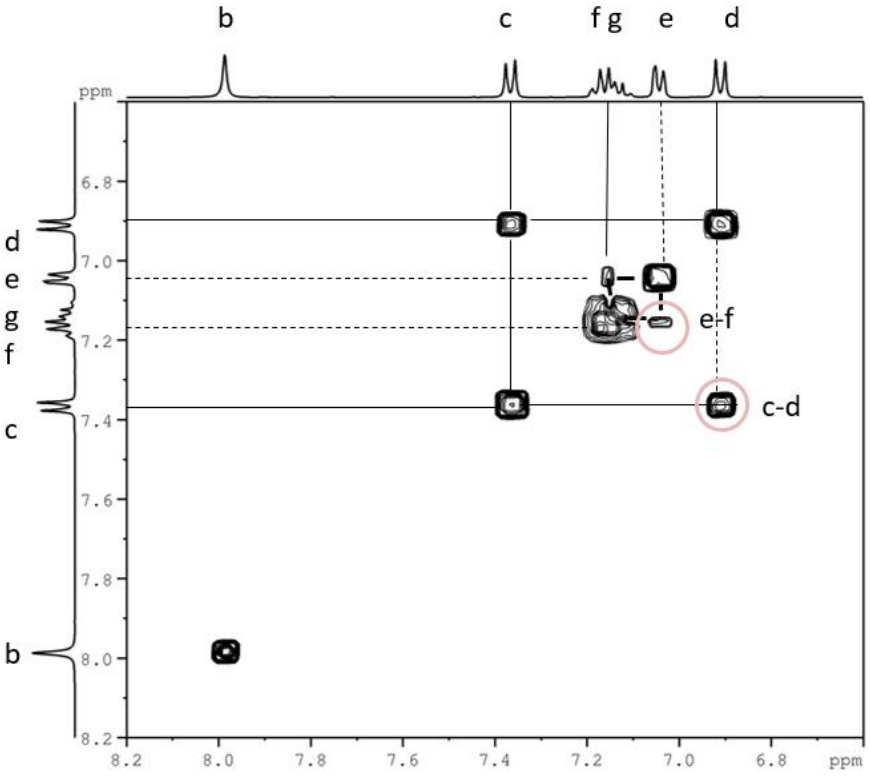

Fig. S5. Partial ^{1}H-^{1}H COSY spectrum of **H_2E** (400 MHz, 298 K, DMSO-d_6).

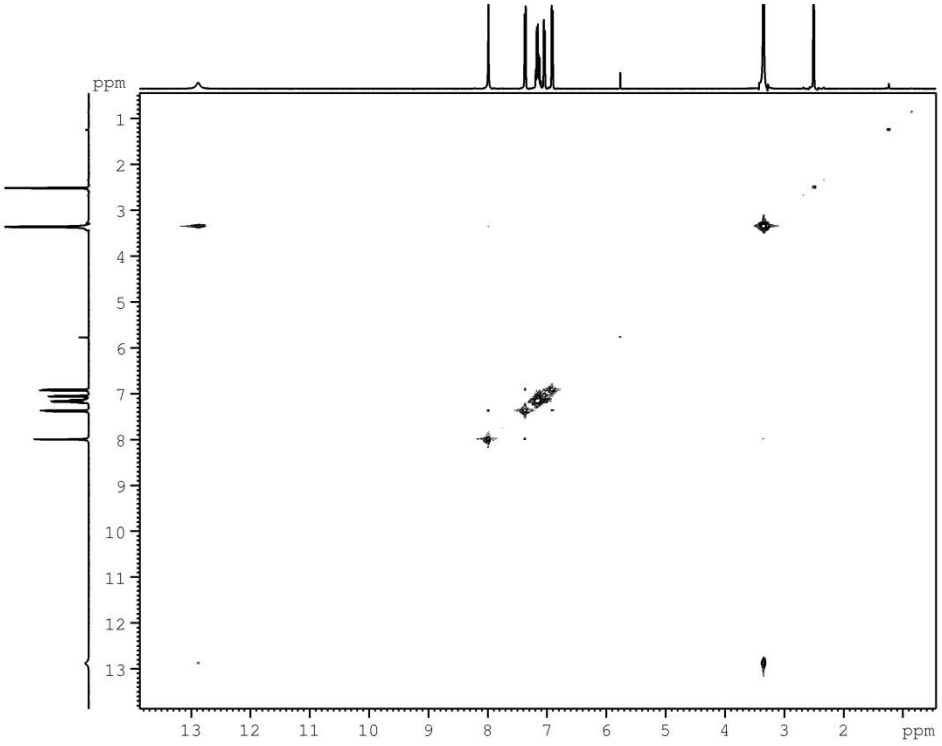

Fig. S6. Full ^{1}H-^{1}H NOESY spectrum of **H_2E** (400 MHz, 298 K, DMSO-d_6)

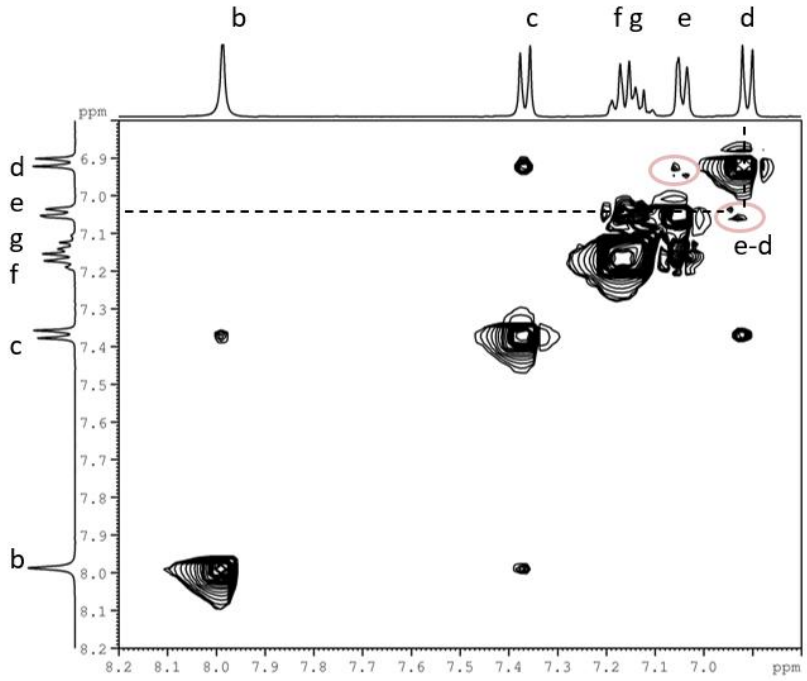

Fig. S7. Partial ^{1}H-^{1}H NOESY spectrum of **H_2E** (400 MHz, 298 K, DMSO-d_6)

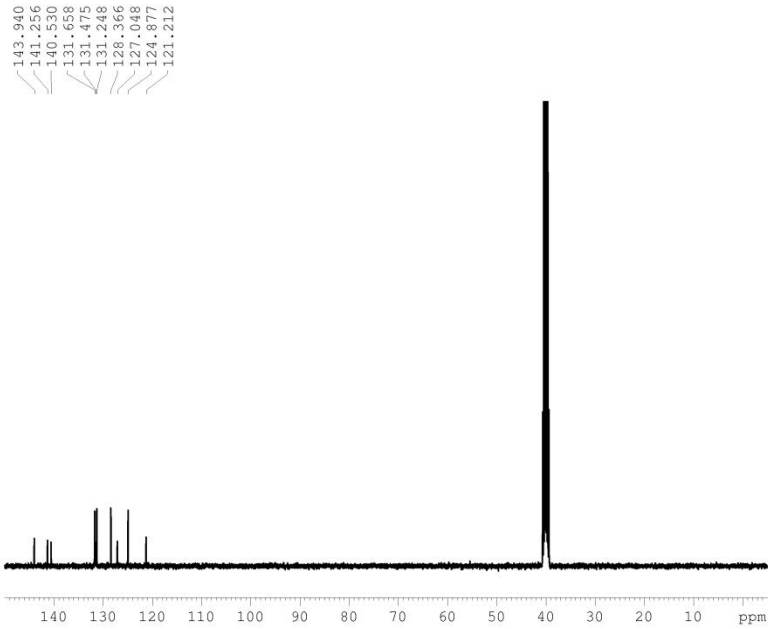

Fig. S8. ^{13}C NMR spectrum of **H_2E** (100 MHz, 298 K, DMSO-d_6) in DMSO-d_6.

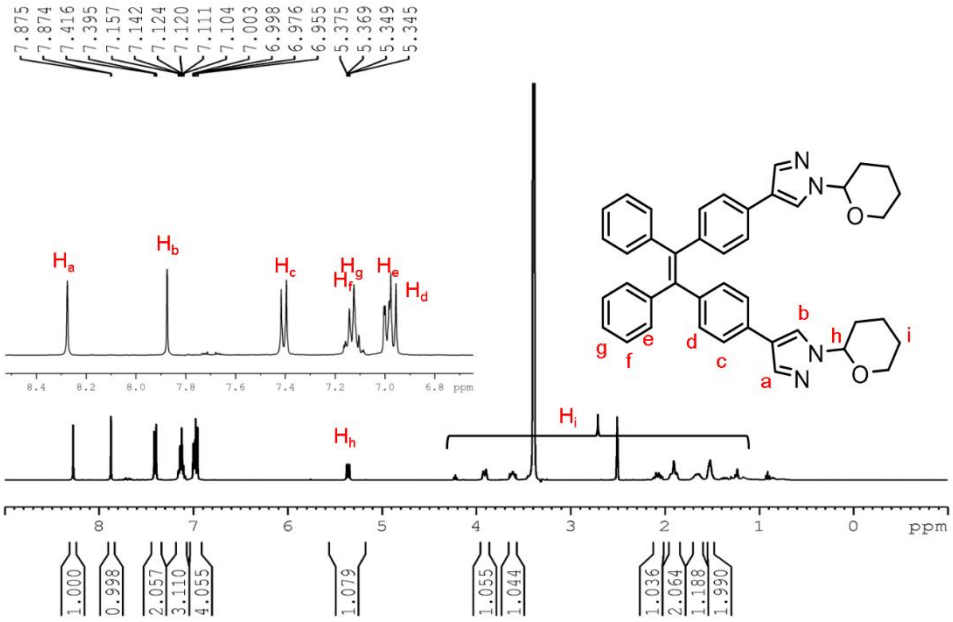

Fig. S9. ^{1}H NMR spectrum of **Z-P** (400 MHz, 298 K, DMSO-d_6).

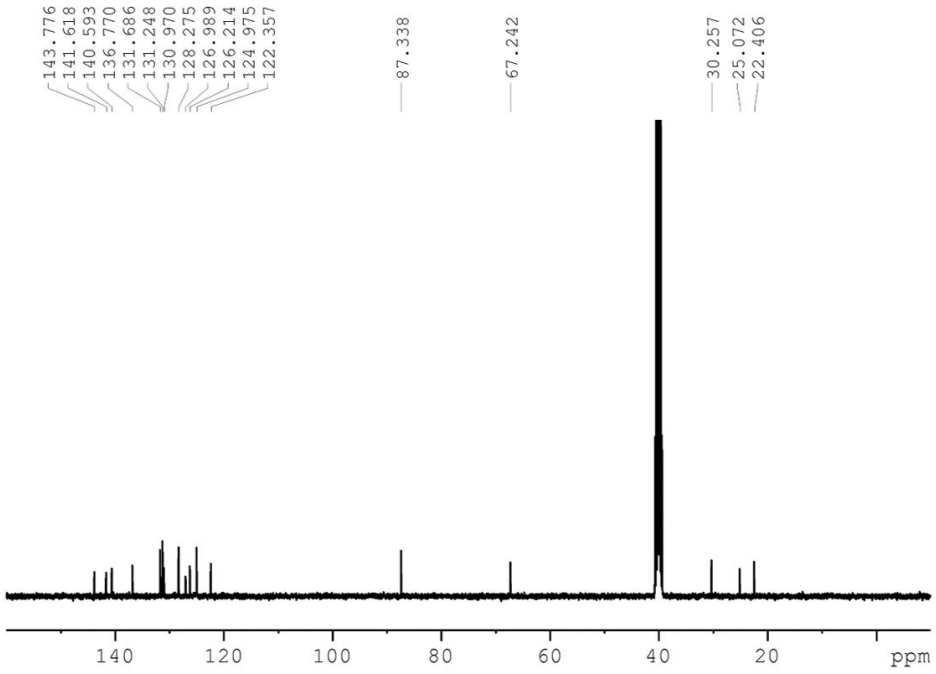

Fig. S10. ^{13}C NMR spectrum of **Z-P** (100 MHz, 298 K, DMSO-d_6).

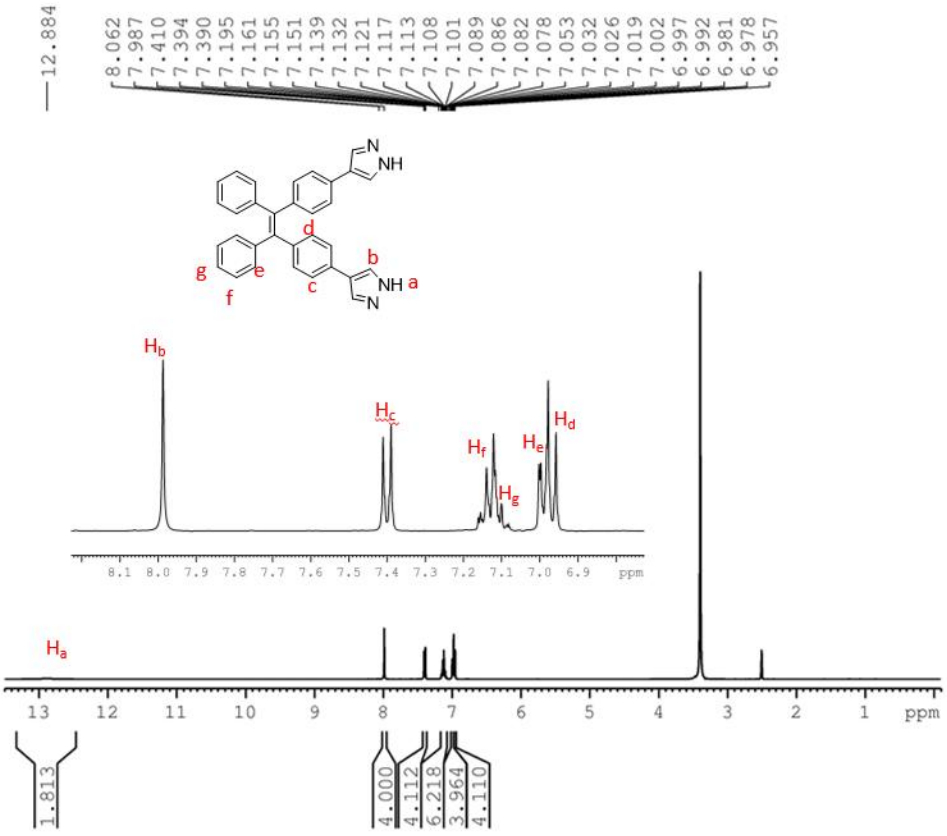

Fig. S11. ^{1}H NMR spectrum of **H_2Z** in (400 MHz, 298 K, DMSO-d_6)

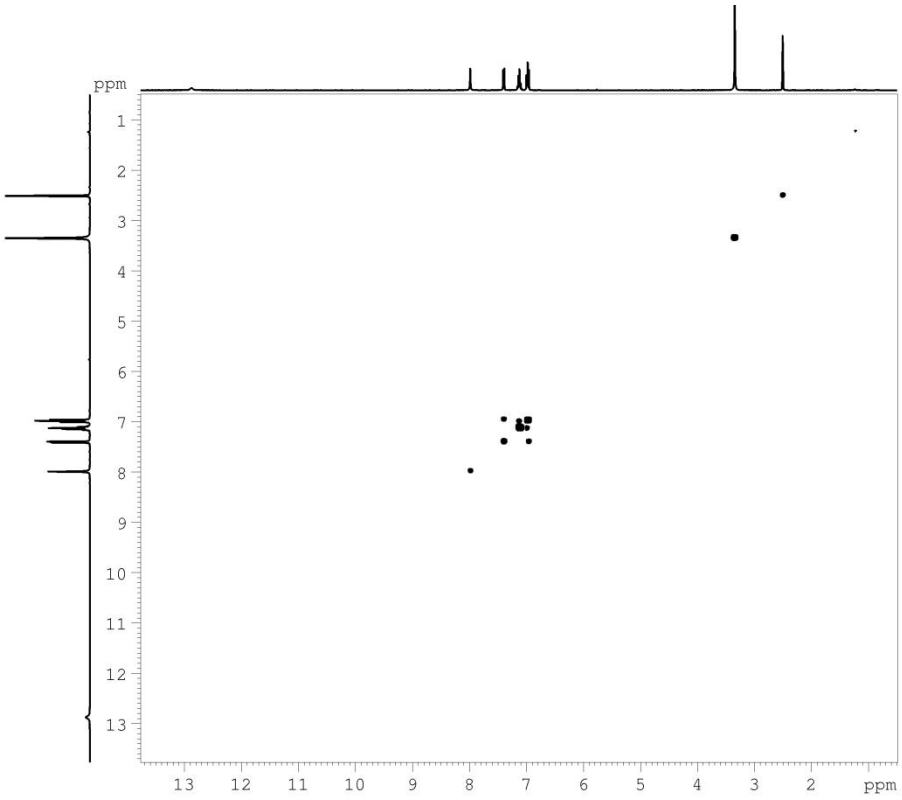

Fig. S12. Full ^{1}H-^{1}H COSY spectrum of **H_2Z** (400 MHz, 298 K, DMSO-d_6)

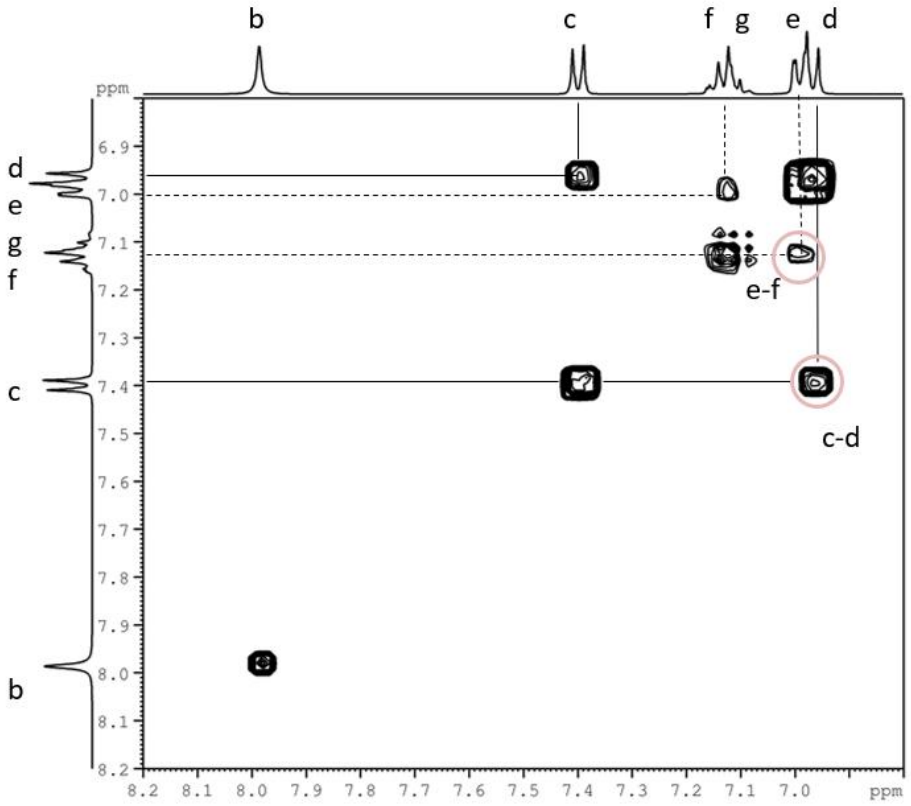

Fig. S13. Partial ^{1}H-^{1}H COSY spectrum of **H_2Z** (400 MHz, 298 K, DMSO-d_6).

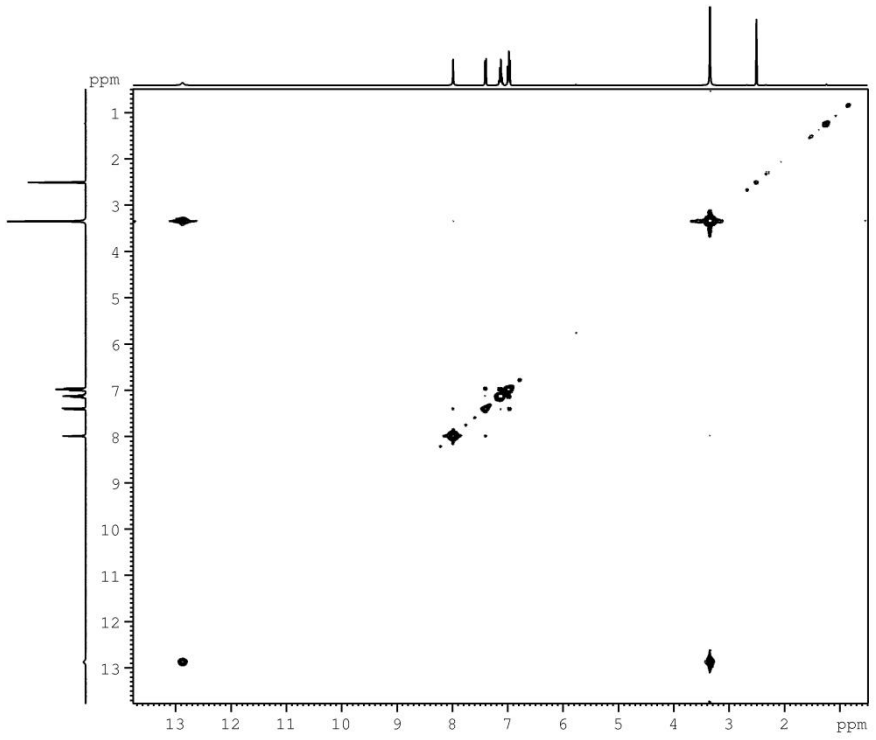

Fig. S14. Full ^{1}H-^{1}H NOESY spectrum of **H_2Z** (400 MHz, 298 K, DMSO-d_6)

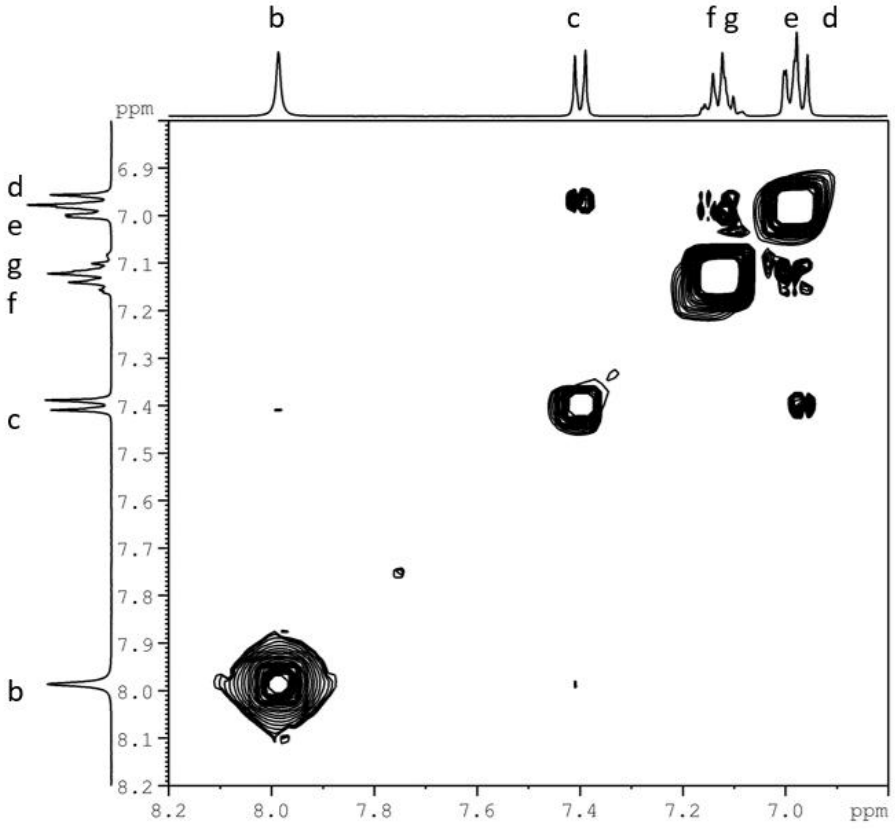

Fig. S15. Partial ^{1}H-^{1}H NOESY spectrum of **H_2Z** (400 MHz, 298K, DMSO-d_6)

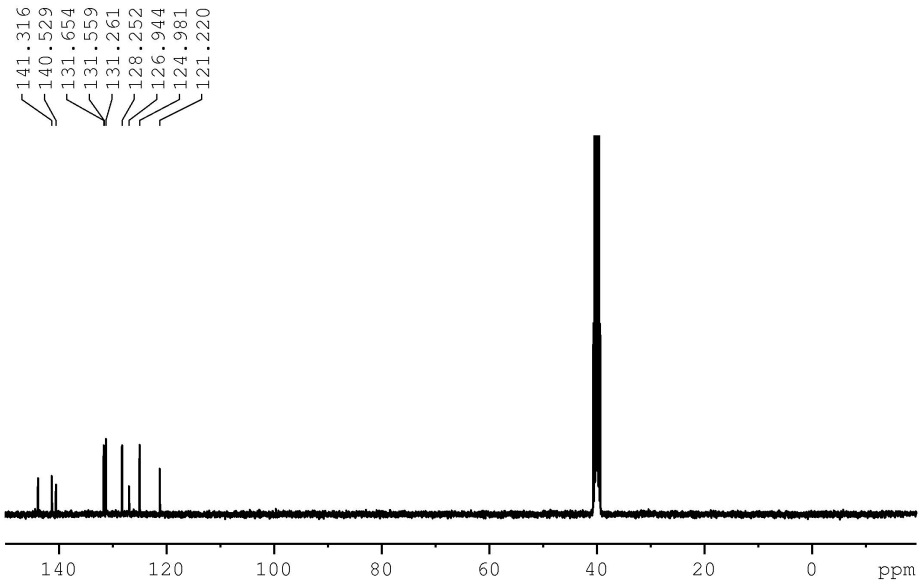

Fig. S16. ^{13}C NMR spectrum of **H_2Z** (100 MHz, 298 K, DMSO-d_6)

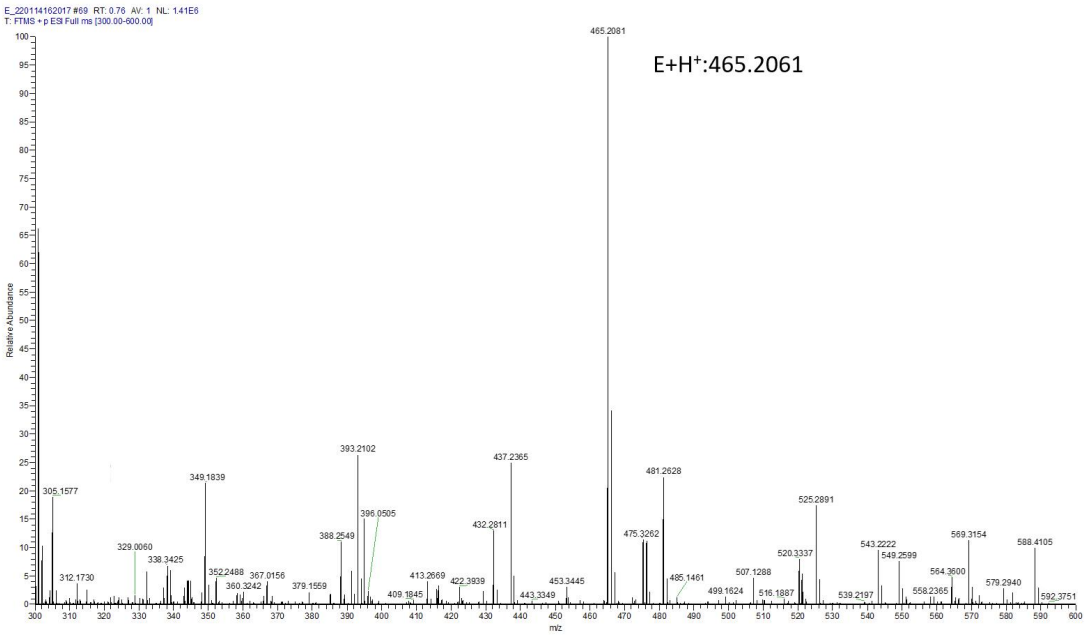

Fig. S17. FT-MS spectrum of **H_2E** in methanol.

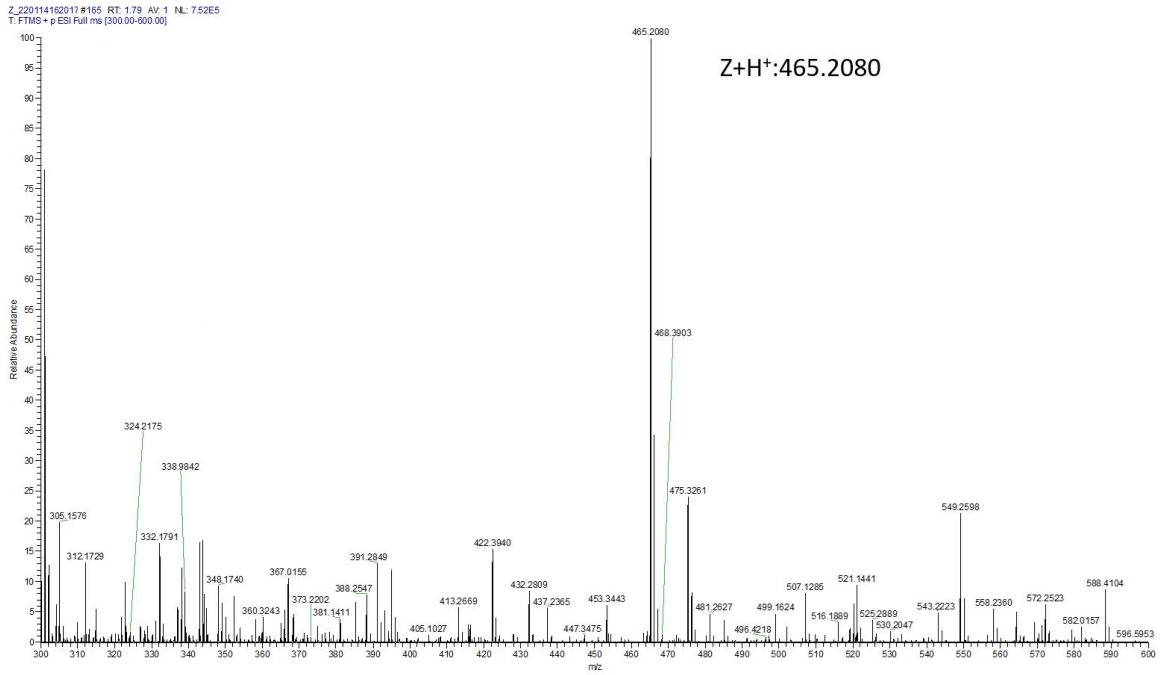

Fig. S18. FT-MS spectrum of **H_2Z** in methanol.

4. Synthesis and characterization of supramolecular metallacycles

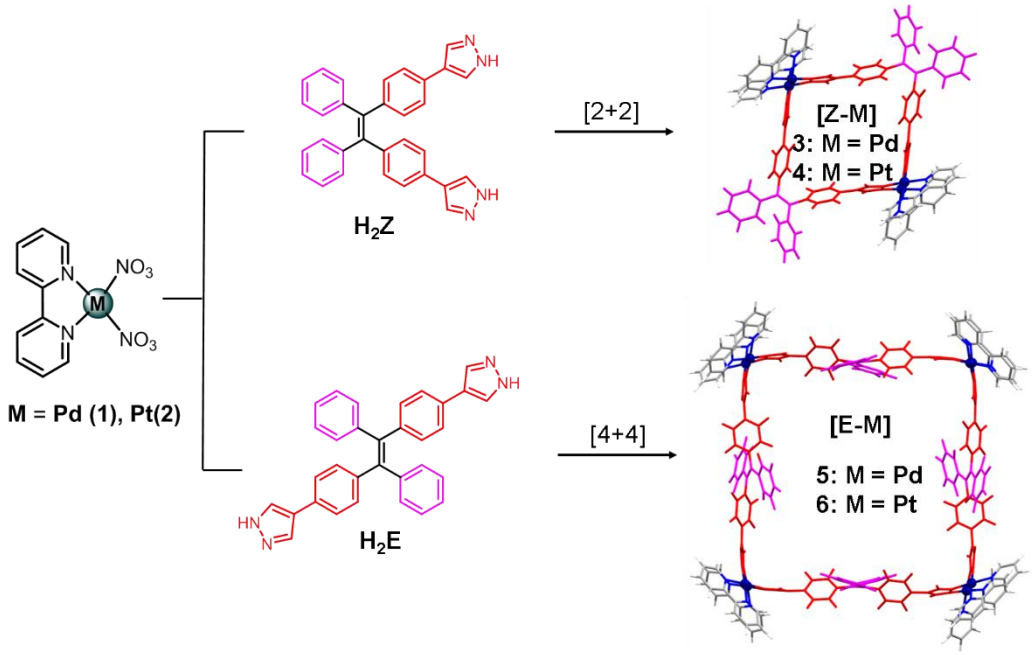

Scheme S2. Schematic representation of the formation of discrete metallacycles.

Self-assembly of metallacycles: A mixture of ligand (H_2E or H_2Z) (4.6 mg, 0.01 mmol) and $[(bpy)_2M_2(NO_3)_2](NO_3)_2$ (0.01 mmol) (M = Pd, Pt) was stirred vigorously in 1 ml DMSO-d_6 at room temperature overnight. ^{1}H NMR, ^{1}H-^{1}H COSY and ^{1}H-^{1}H NOESY spectroscopy confirmed quantitative formation of metallacycles. Some of these products have gained crystal by EA diffused into DMSO. These crystals are both yellow crystals and suitable for X-ray analysis. Anion exchange was conducted to modify solubility of the products in different solvents; thus, treatment with excess KPF_6 (10 equiv. of NO_3^-) to precipitate the complexes with PF_6^- as counterions.

[E-Pd]: yield: 95%. ^{1}H NMR (400 MHz, DMSO-d_6, 298 K): δ(ppm) 8.72-8.74 (d, 4H, J = 8.62 Hz), 8.44-8.48 (t, 4H), 8.39 (s, 4H), 8.26-8.39 (t, 4H), 7.78-7.81 (t, 4H),7.39-7.42(t,4H) 7.07-7.16 (m, 6H), 6.99-7.01 (t, 4H), 6.92-6.94 (d, 4H)

ESI-MS (acetonitrile) m/z: Anal. Calcd for $[(E\text{-}Pd)\text{-}3(PF_6)]^{3+}$: 1558.64, Found：1158.21.

[E-Pt]: yield: 71%. ^{1}H NMR (400 MHz, DMSO-d_6, 298 K): δ(ppm) 8.73-8.75 (d, 4H, J = 8.26 Hz), 8.46-8.66(m, 12H), 7.82-7.85(t, 4H), 7.47 (s, 4H), 7.13-7.17 (m, 6H), 7.0-7.04 (m, 4H),6.94-6.97(m, 4H).

ESI-MS (acetonitrile) m/z: Anal. Calcd for $[(E\text{-}Pt)\text{-}3(PF_6)]^{3+}$: 1794.56, Found: 1794.28.

[Z-Pd]: yield: 97%. ^{1}H NMR (400 MHz, DMSO-d_6, 298 K): δ(ppm) 8.70-8.72 (d, 4H, J=8.42 Hz), 8.42-8.46(t, 4H), 8.34 (s, 4H), 8.19-8.20(t, 4H), 7.75-7.78 (t, 4H), 7.41-7.43 (d, 4H), 7.12-7.19 (m, 6H), 7.07-7.09 (d, 4H), 6.95-6.97 (d, 4H).

ESI-MS (acetonitrile) m/z: Anal. Calcd. for $[(Z\text{-}Pd)\text{-}2(PF_6)]^{2+}$: 1132.38, Found: 1132.17; $[(Z\text{-}Pd)\text{-}3(PF_6)]^{3+}$: 706.58, Found: 706.79; $[(Z\text{-}Pd)\text{-}4(PF_6)]^{4-}$:493.70, Found: 494.09.

[Z-Pt]: yield: 78%. ^{1}H NMR (400 MHz, DMSO-d_6, 298 K): δ(ppm) 8.72-8.74 (d, 4H, J=8.62 Hz), 8.47-8.55(m, 12H), 7.79-7.82(t, 4H), 7.46-7.48 (d, 4H), 7.15-7.18 (m, 6H), 7.09-7.11 (d, 4H), 6.96-6.98 (d, 4H).

ESI-MS (acetonitrile) m/z: $[(Z\text{-}Pt)\text{-}2(PF_6)]^{2+}$: 1310.71, Found: 1310.07; $[(Z\text{-}Pt)\text{-}3(PF_6)]^{3+}$: 824.72, Found: 824.71; $[(Z\text{-}Pt)\text{-}4(PF_6)]^{4+}$: 582.32. Found: 582.31.

5. NMR and MS spectra of supramolecules [E-Pd], [Z-Pd], [E-Pt] and [Z-Pt]

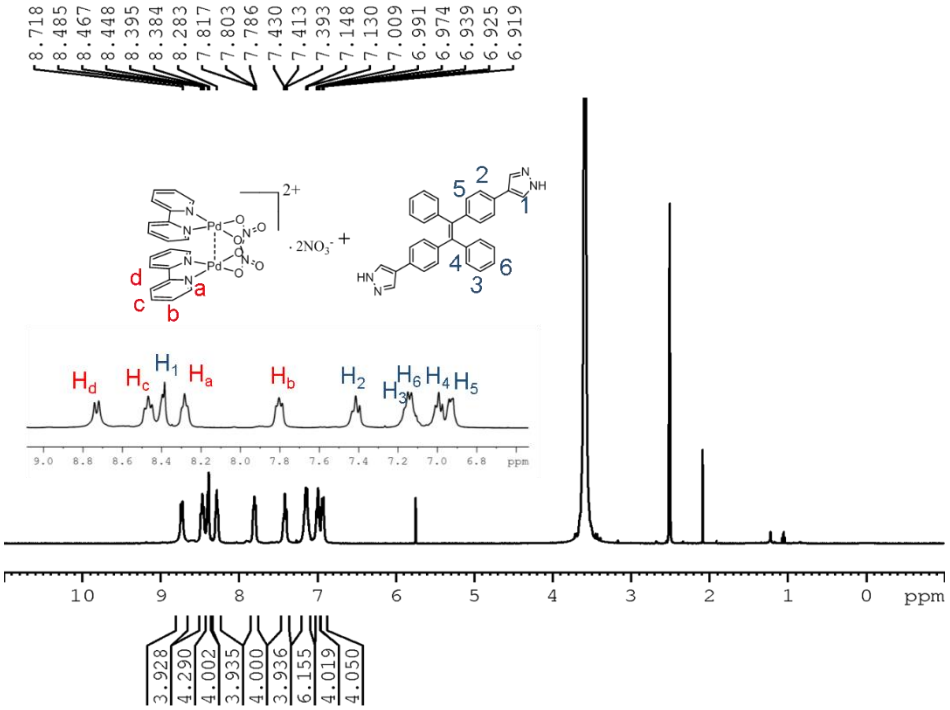

Fig. S19. ^{1}H NMR spectrum of [**E-Pd]** (400 MHz, 298 K, DMSO-d_6)

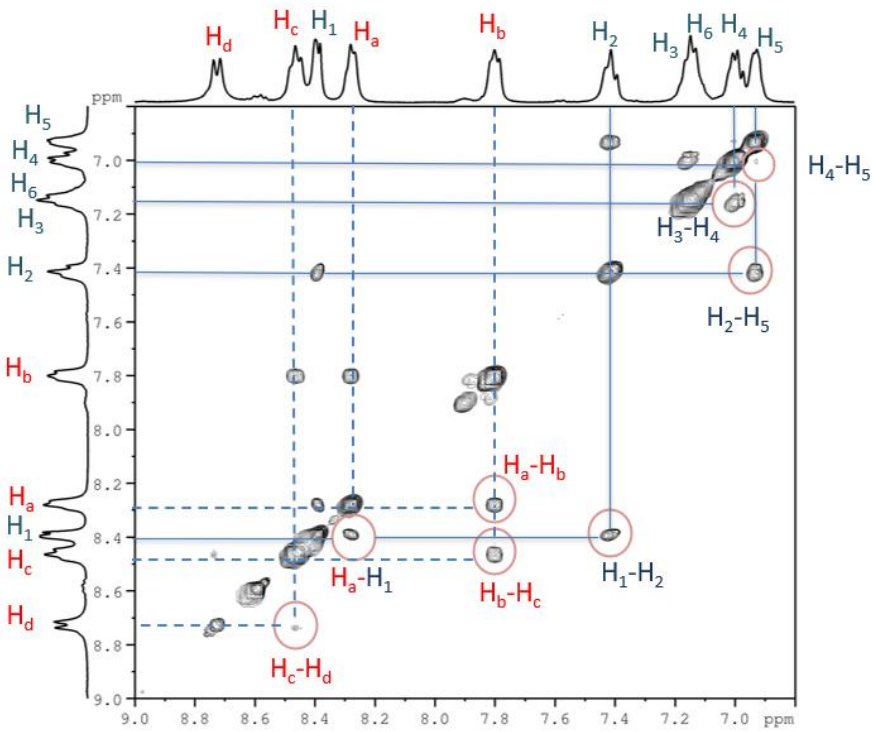

Fig. S20. Partial ^{1}H-^{1}H NOESY spectrum of [**E-Pd]** (400 MHz, 298 K, DMSO-d_6)

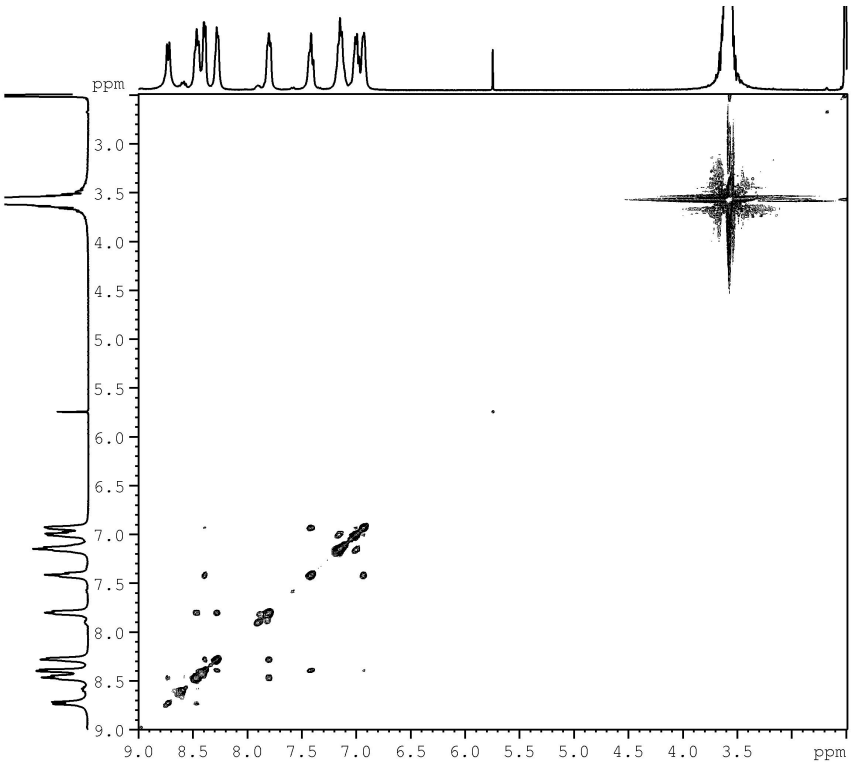

Fig. S21. Full ^{1}H-^{1}H NOESY spectrum of [**E-Pd]** (400 MHz, 298 K, DMSO-d_6).

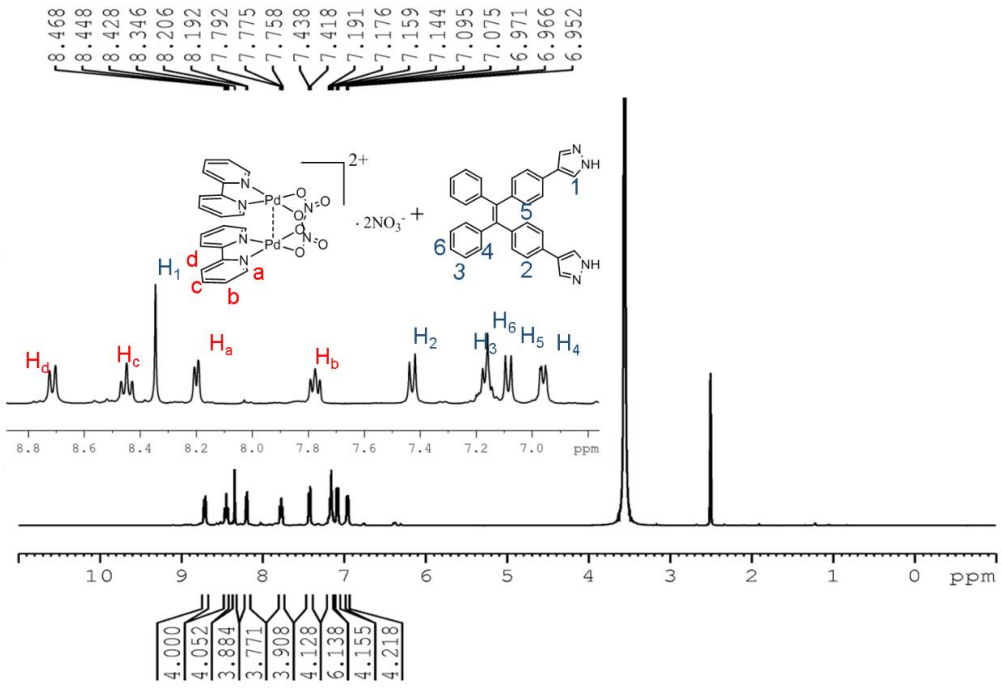

Fig. S22. ^{1}H NMR spectrum of [**Z-Pd]** (400 MHz, 298 K, DMSO-d_6)

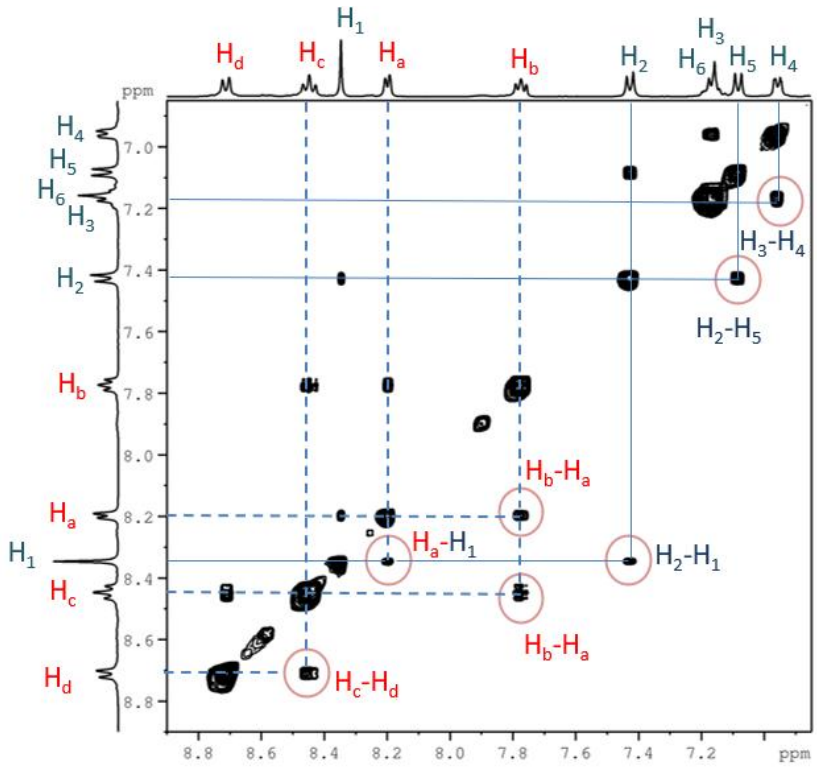

Fig. S23. Partial ^{1}H-^{1}H NOESY spectrum of [**Z-Pd]** (400 MHz, 298 K, DMSO-d_6).

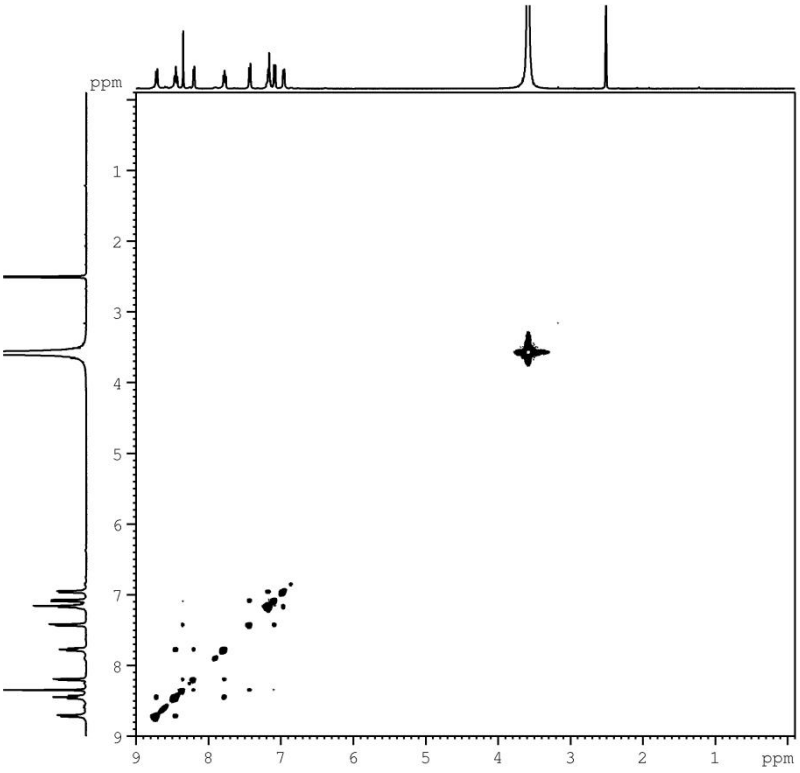

Fig. S24. Full ^{1}H-^{1}H NOESY spectrum of [**Z-Pd]** (400 MHz, 298 K, DMSO-d_6)

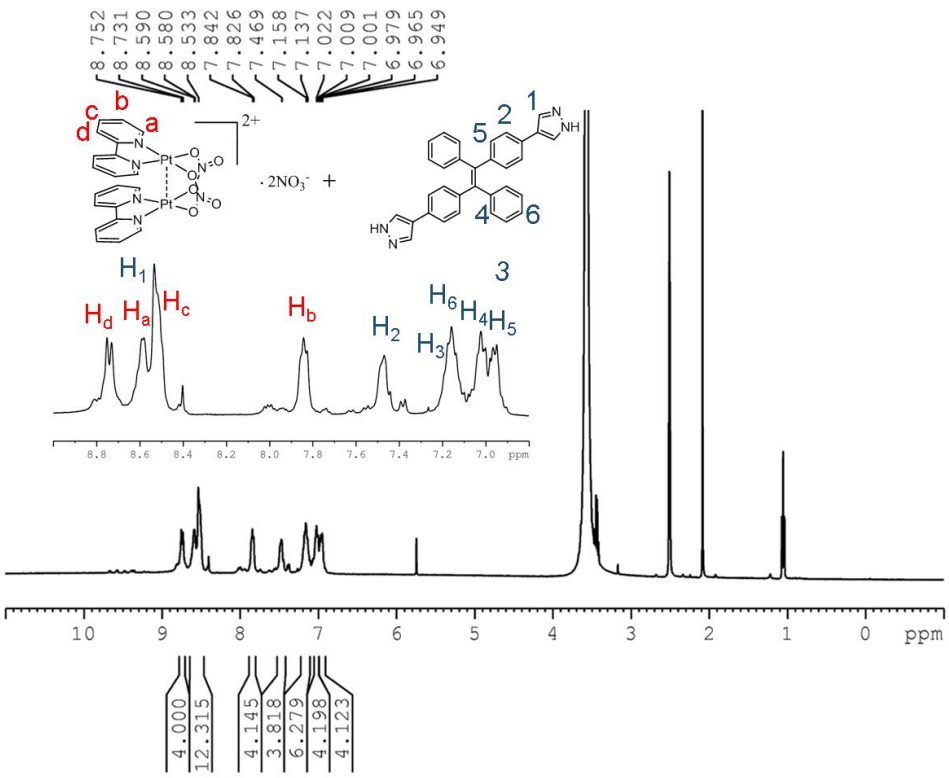

Fig. S25. ^{1}H NMR spectrum of [**E-Pt]** (400 MHz, 298 K, DMSO-d_6)

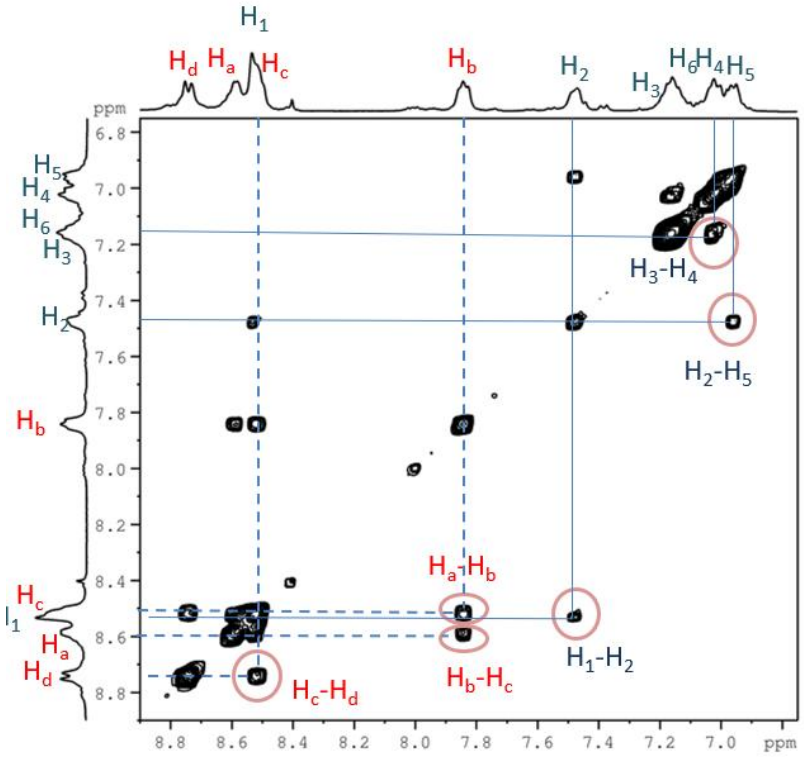

Fig. S26. Partial ^{1}H-^{1}H NOESY spectrum of [**E-Pt]** (400 MHz, 298 K, DMSO-d_6)

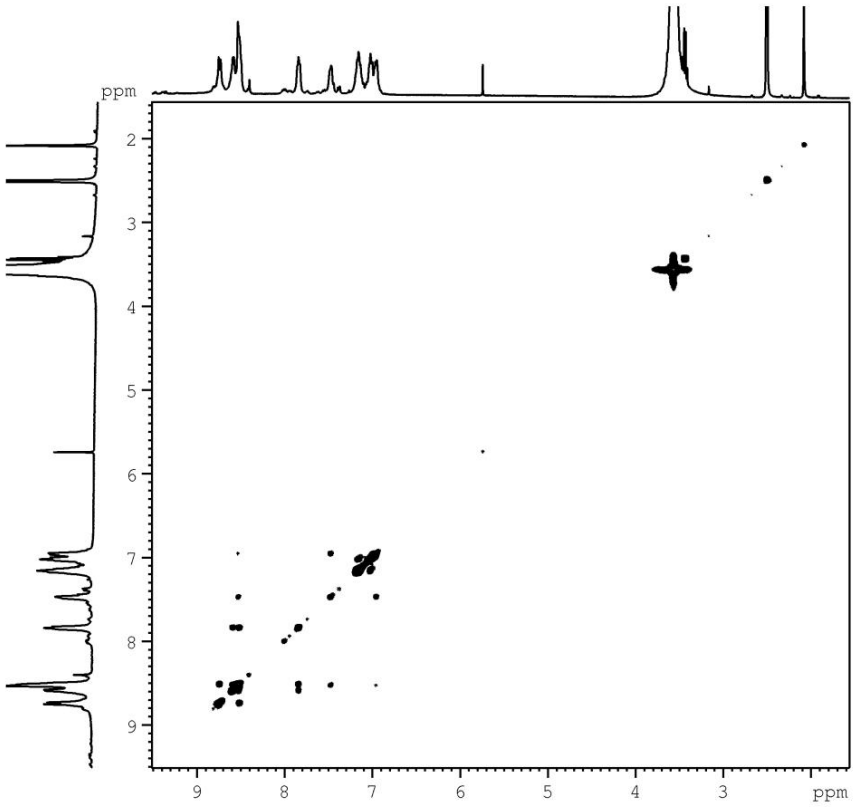

Fig. S27. Full ^{1}H-^{1}H NOESY spectrum of [**E-Pt]** (400 MHz, 298K, DMSO-d_6)

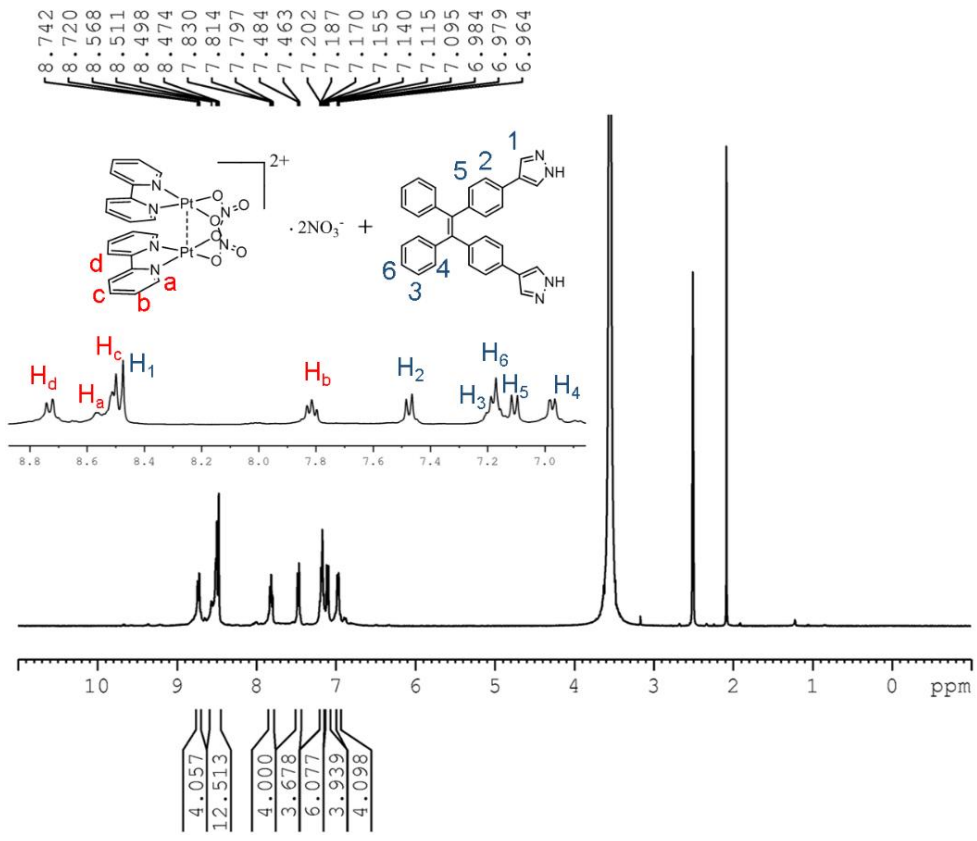

Fig. S28. ^{1}H NMR spectrum of [**Z-Pt]** (400 MHz, 298K, DMSO-d_6)

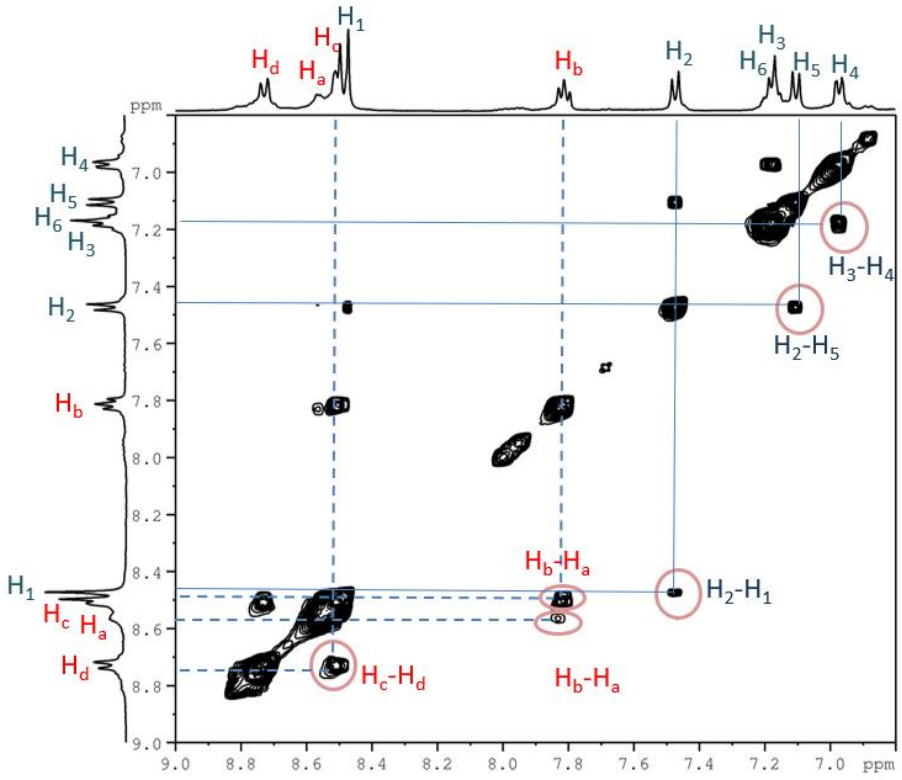

Fig. S29. Partial ^{1}H-^{1}H NOESY spectrum of **[Z-Pt]** (400 MHz, 298K, DMSO-d_6)

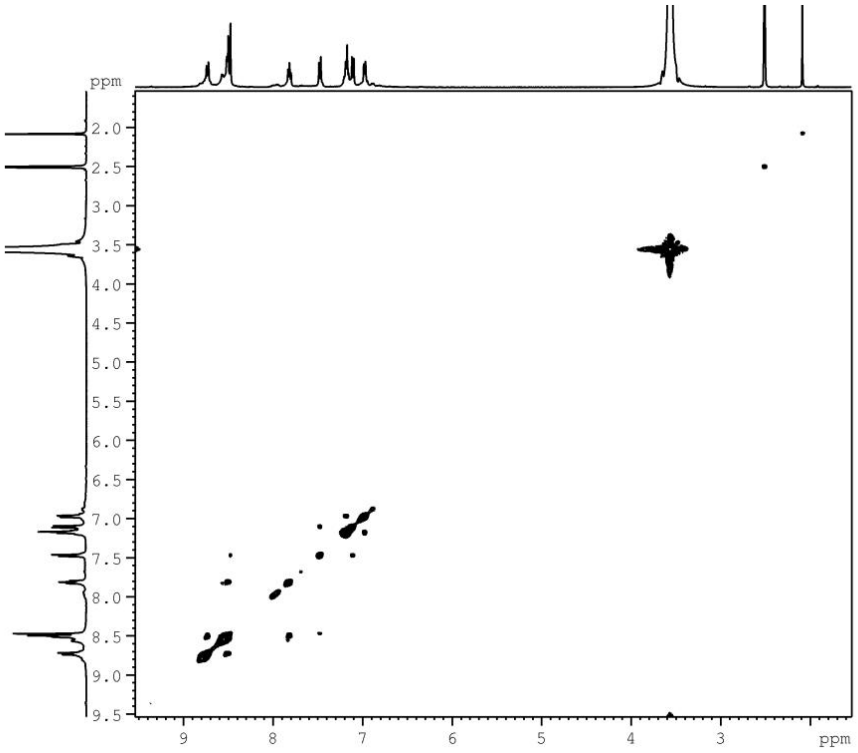

Fig. S30. Full ^{1}H-^{1}H NOESY spectrum of **[Z-Pt]** (400 MHz, 298K, DMSO-d_6)

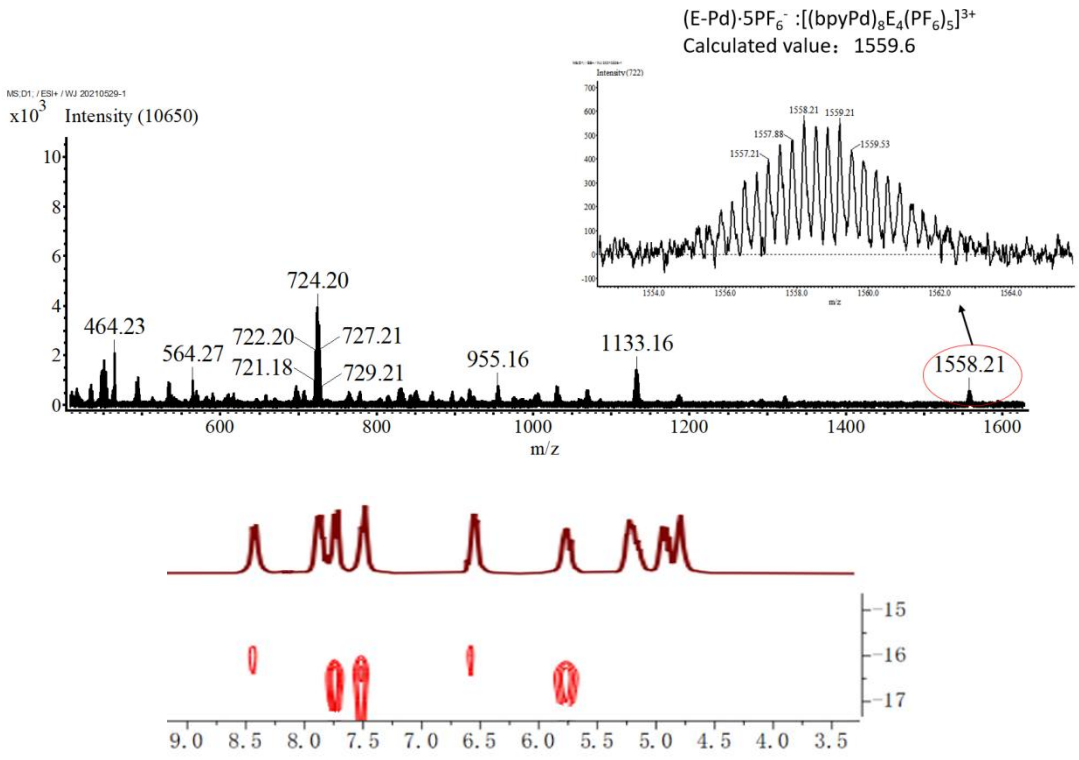

Fig.S31. ESI-MS spectra of [**E-Pd**]·**8PF$_6$** in acetonitrile and superimposed ^{1}H DOSY spectra of [Z-Pd] in DMSO-d$_6$.

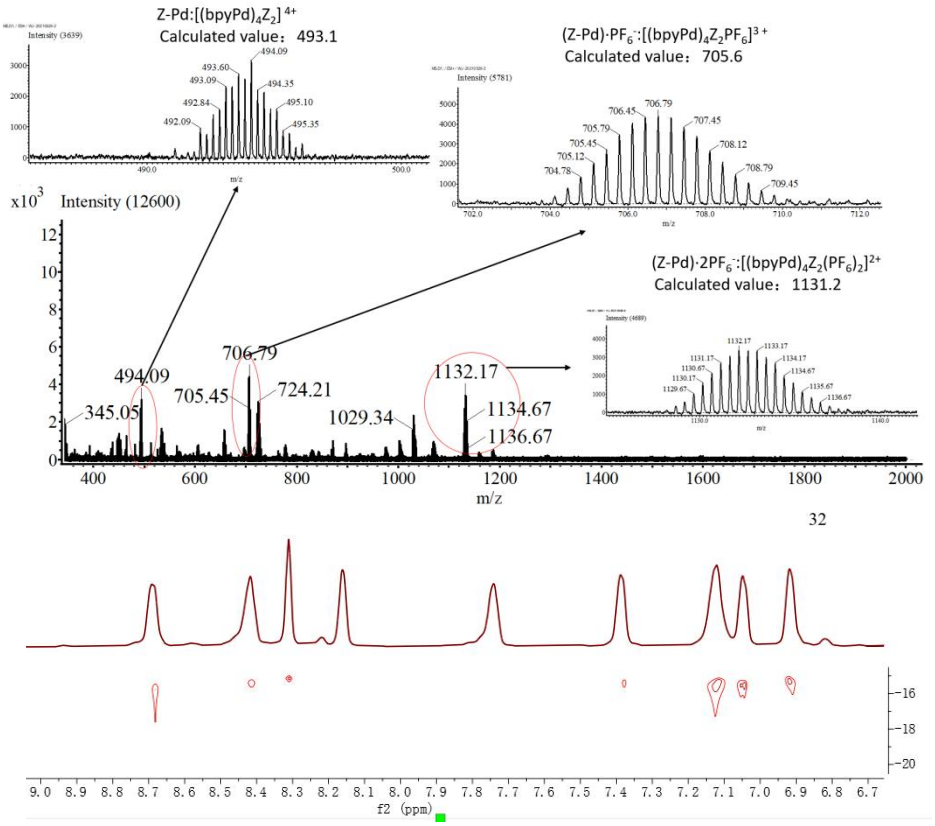

Fig. S32. ESI-MS spectra of [**Z-Pd**]·**4PF$_6$** in acetonitrile and superimposed ^{1}H DOSY spectra of [Z-Pd] in DMSO-*d*$_6$.

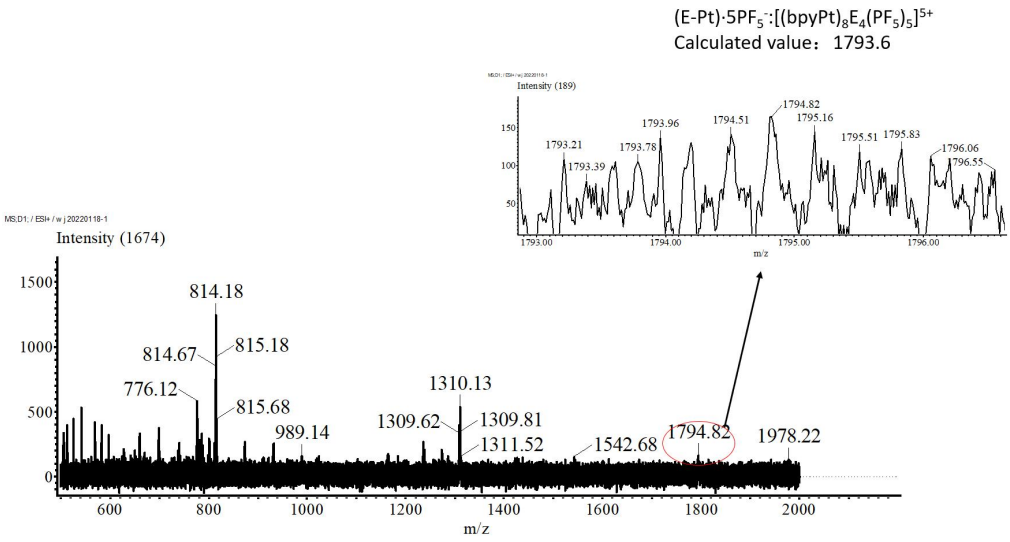

Fig. S33. ESI-MS spectra of [**E-Pt**]·**8PF$_6$** in acetonitrile.

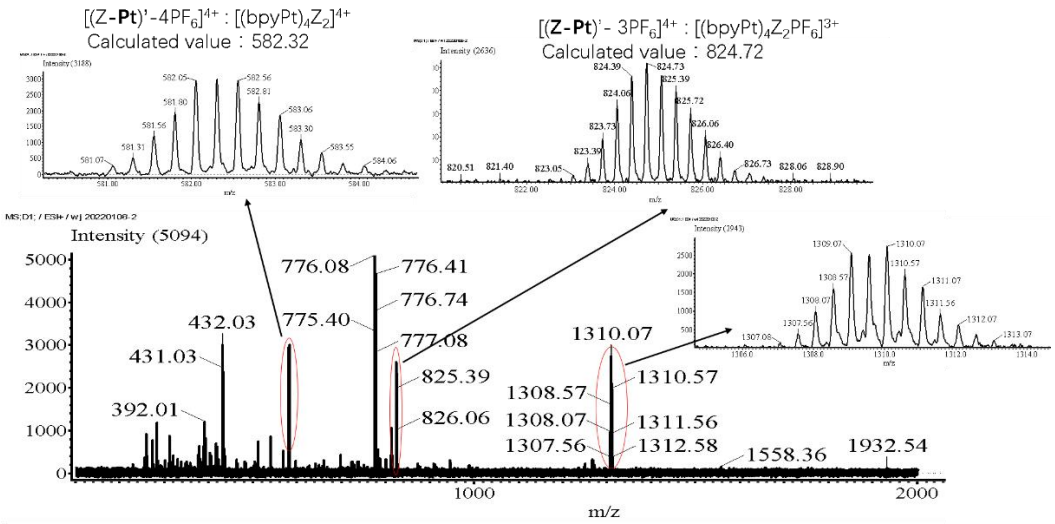

Fig. S34. ESI-MS spectra of [**Z-Pt**]·**4PF$_6$** in acetonitrile.

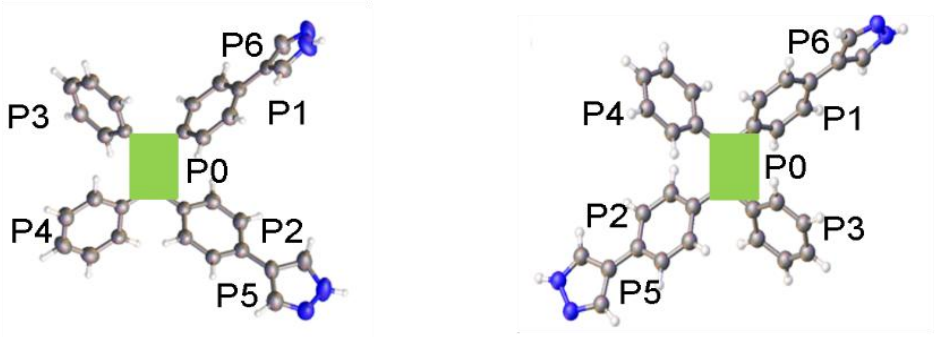

Table S1. Dihedral angles (°) between the π-conjugate systems in **H$_2$E**, **H$_2$Z**, [**E-Pt**], and [**Z-Pt**] in the single crystal and simulated structures.

Dihedral angle		H_2Z	[Z-Pt]	H_2E	[E-Pt]
P1	P0	46.17	56.59	39.08	46.36
P2		51.98	46.56	57.45	45.38
P3		47.38	40.00	53.16	14.21
P4		54.80	61.43	43.47	14.70
P1	P6	5.67	20.20	9.91	42.95
P2	P5	18.48	36.30	7.90	39.18
P5	P6	67.79	79.86	85.22	13.64
P3	P4	59.25	58.85	83.57	28.91
P1	P2	56.75	59.35	83.48	88.32

6. Identification and characterization of stereoisomers during the synthesis of ligand H_2Z and H_2E.

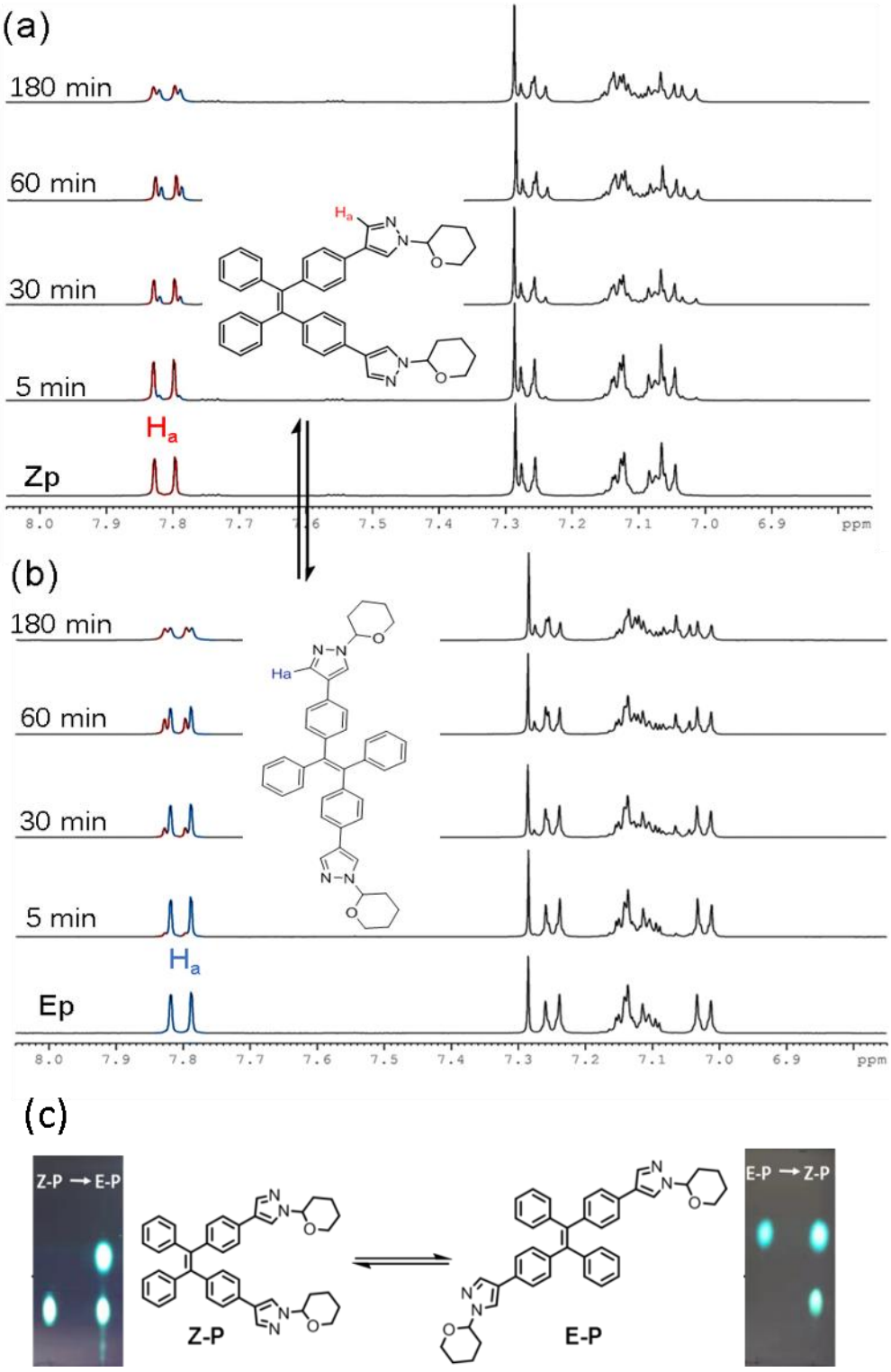

Fig. S35. ^{1}H NMR spectra of **Z-P** and **E-P** after different irradiation (λ = 365 nm) (400 MHz, 298K, DMSO-d_6).

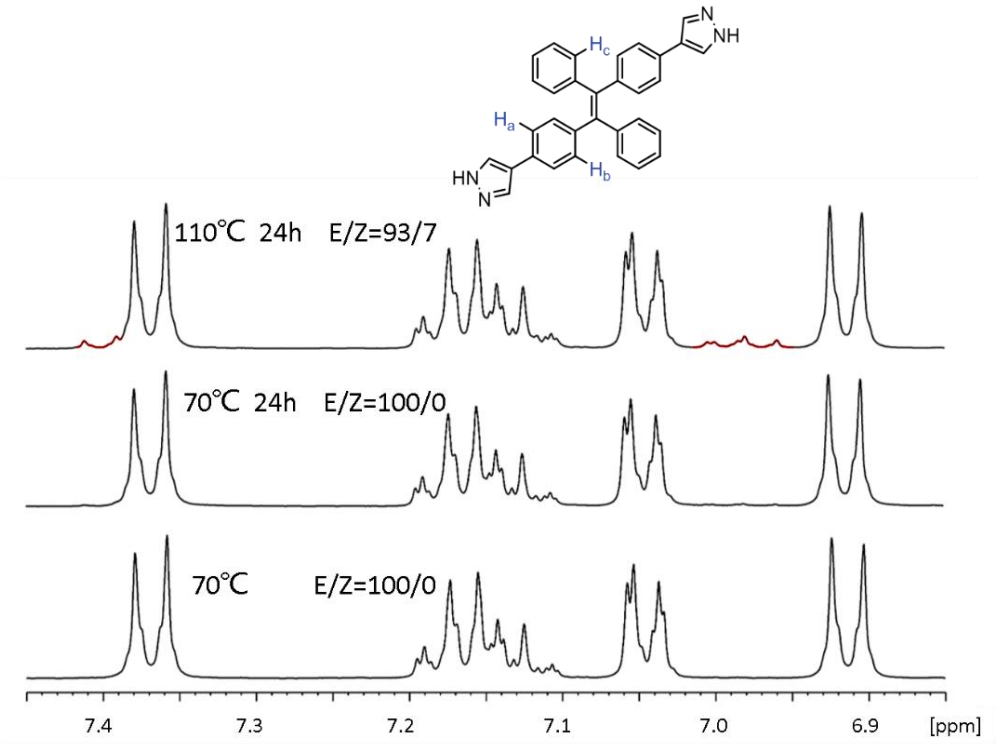

Fig. S36. ^{1}H NMR spectra of **H_2E** after heating (400 MHz, 298 K, DMSO-d_6).

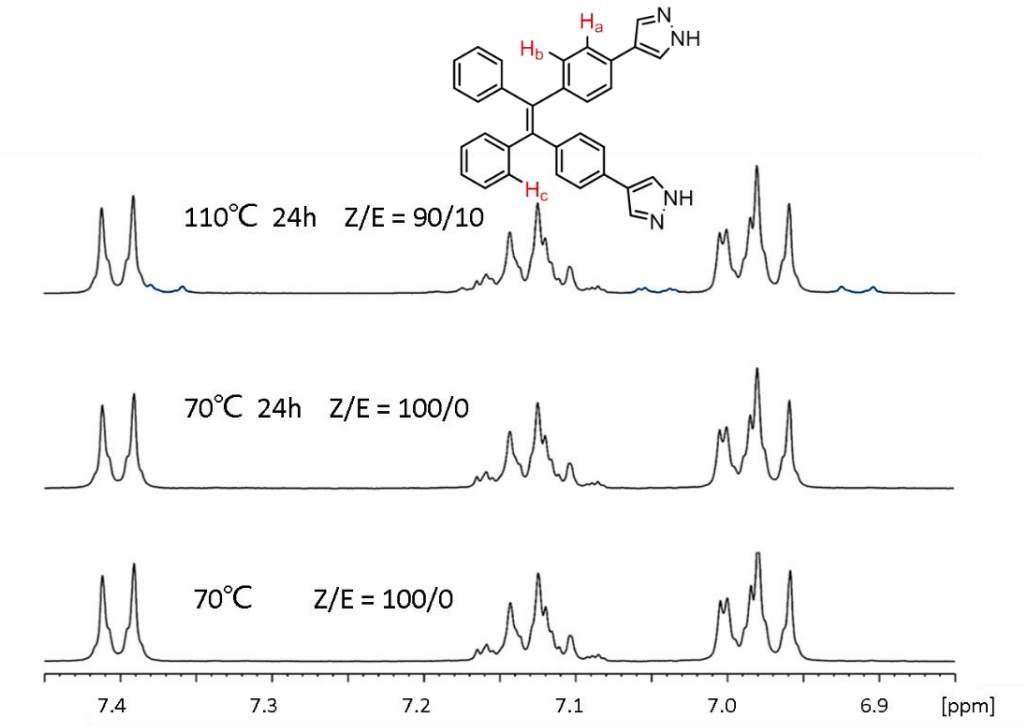

Fig. S37. ^{1}H NMR spectra of **H_2Z** after heating (400 MHz, 298K, DMSO-d_6).

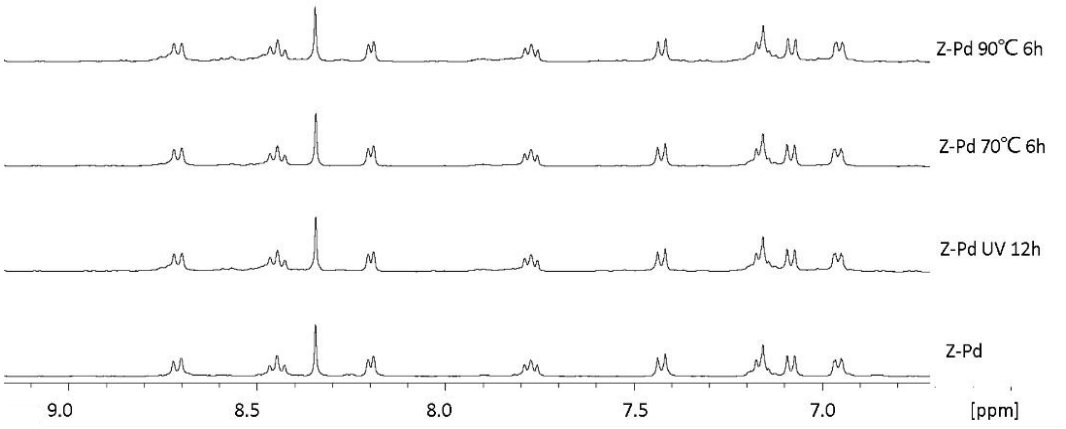

Fig. S38. ^{1}H NMR spectra of **[Z-Pd]** at different conditions (400 MHz, 298K, DMSO-d_6)

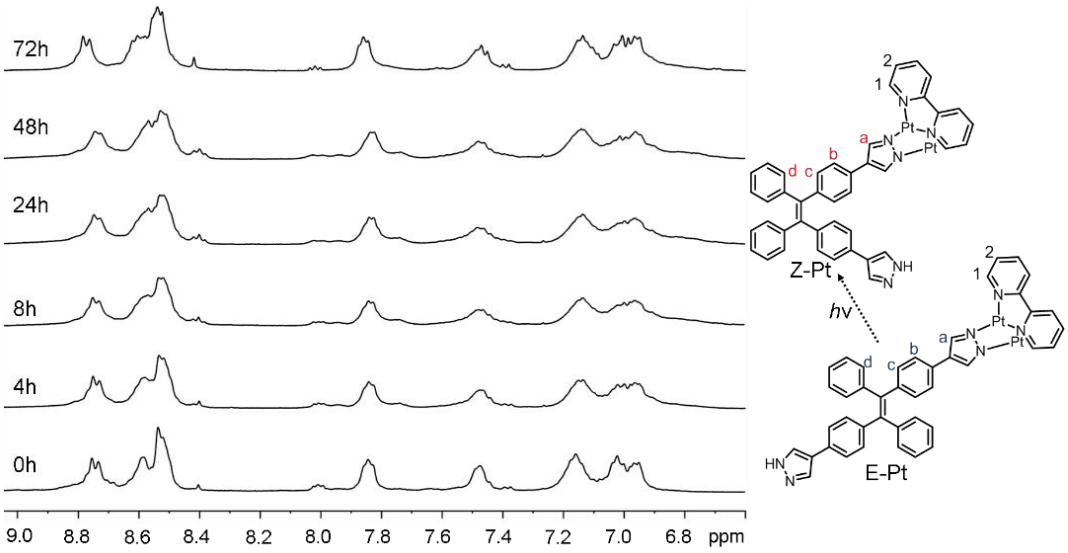

Fig. S39. ^{1}H NMR spectra of **[E-Pt]** by irradiation (λ = 365 nm) at different time (400 MHz, 298 K, DMSO-d_6)

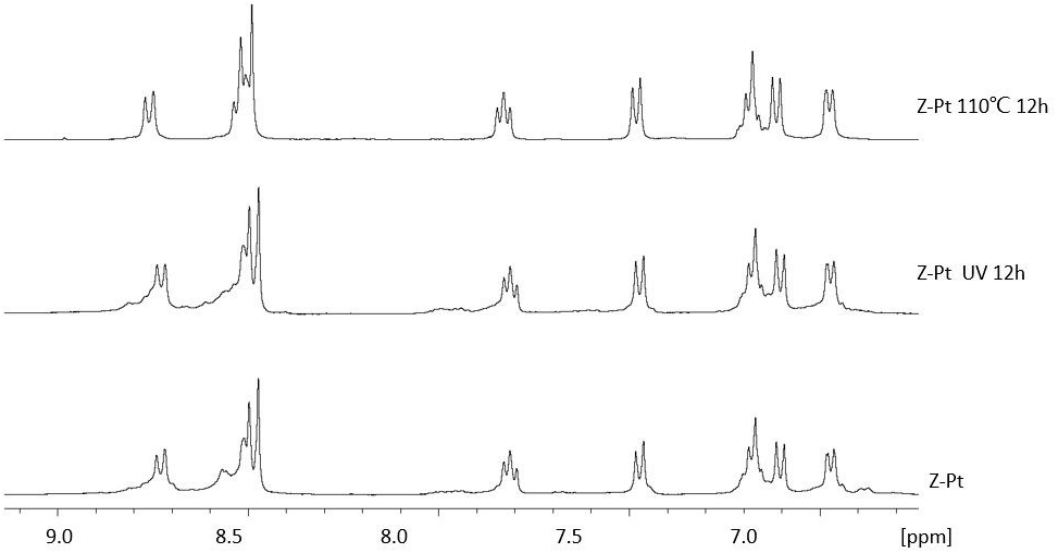

Fig. S40. [1]H NMR spectra of **[Z-Pt]** at different conditions (400 MHz, 298 K, DMSO-d_6)

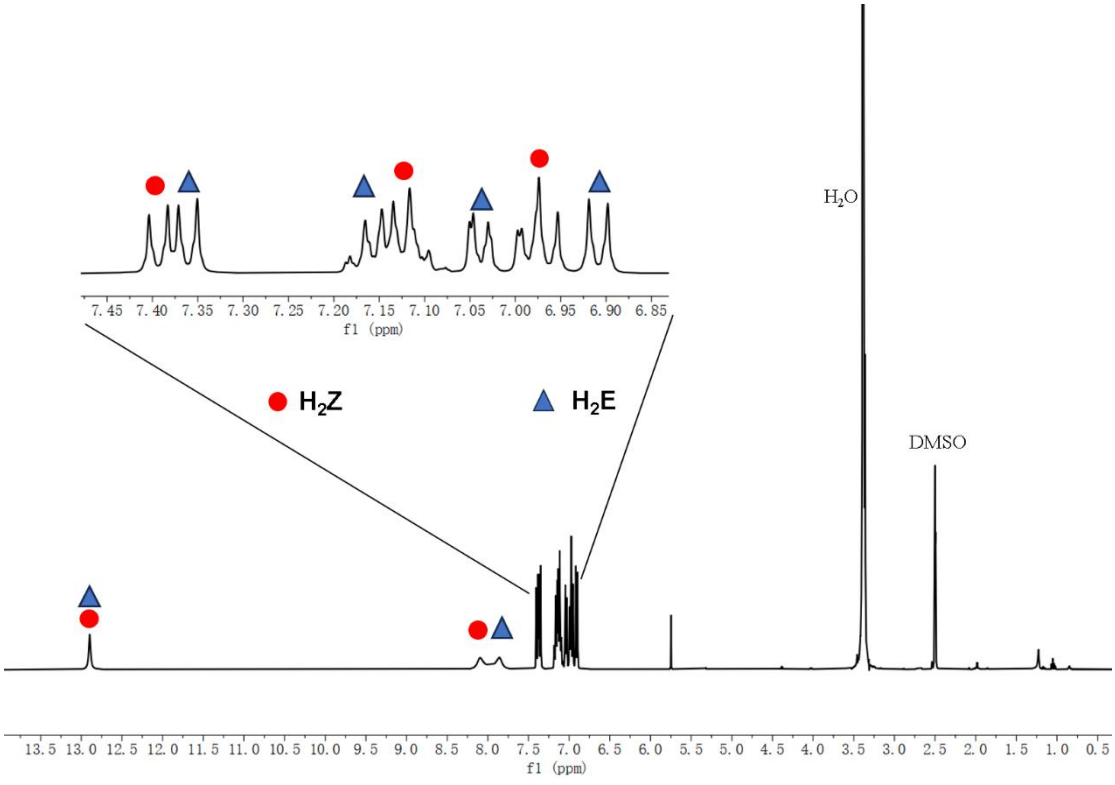

Fig. S41. [1]H NMR spectrum of the isomer mixture **H_2E**/**H_2Z** (400 MHz, 298K, DMSO-d_6).

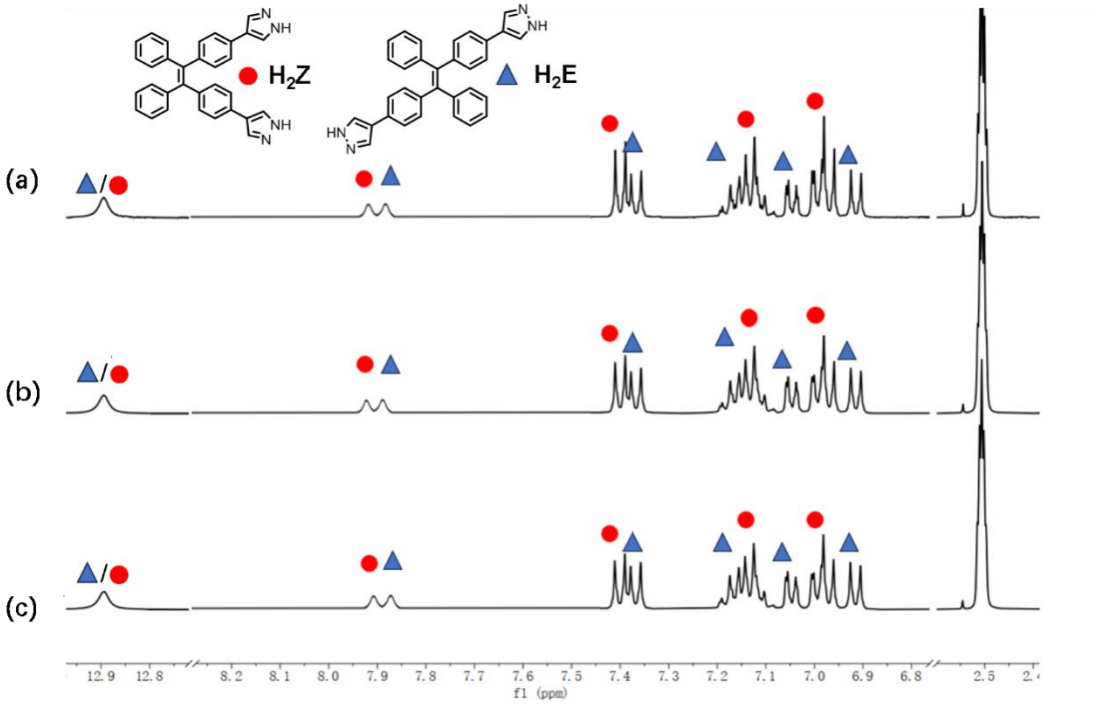

Fig. S42. ^{1}H NMR spectra of the isomer mixture **H_2E**/**H_2Z** before (a) and after irradiation (λ = 365 nm) for 12 h (b) and 24 h (c) (400 MHz, 298K, DMSO-d_6).

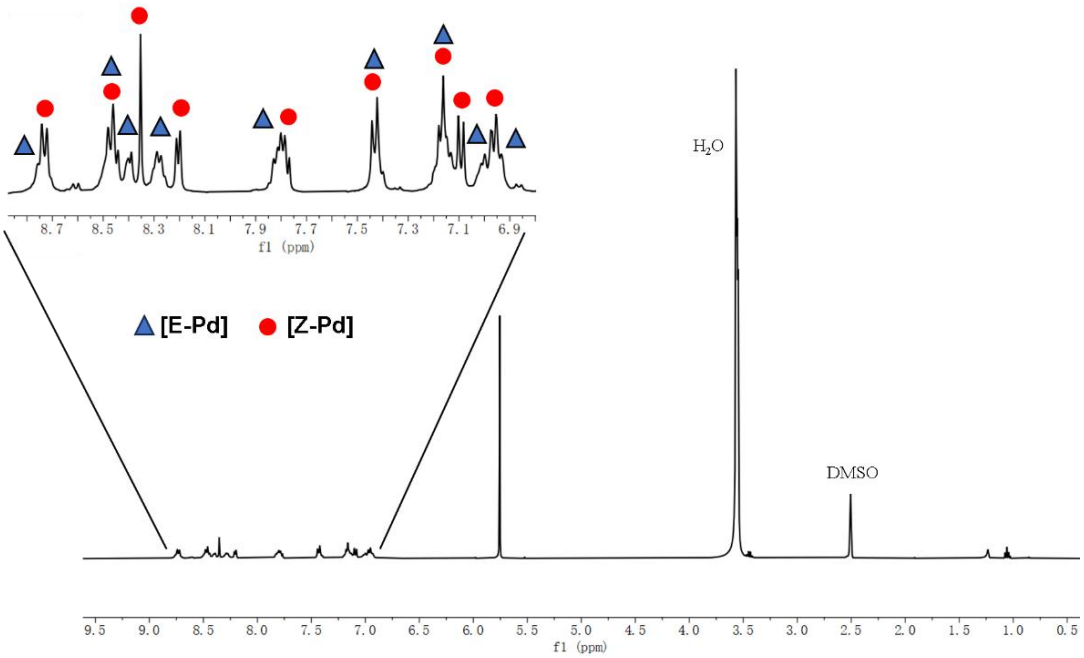

Fig. S43. ^{1}H NMR spectrum of mixture **[Z-Pd]/[E-Pd]** (400 MHz, 298K, DMSO-d_6)

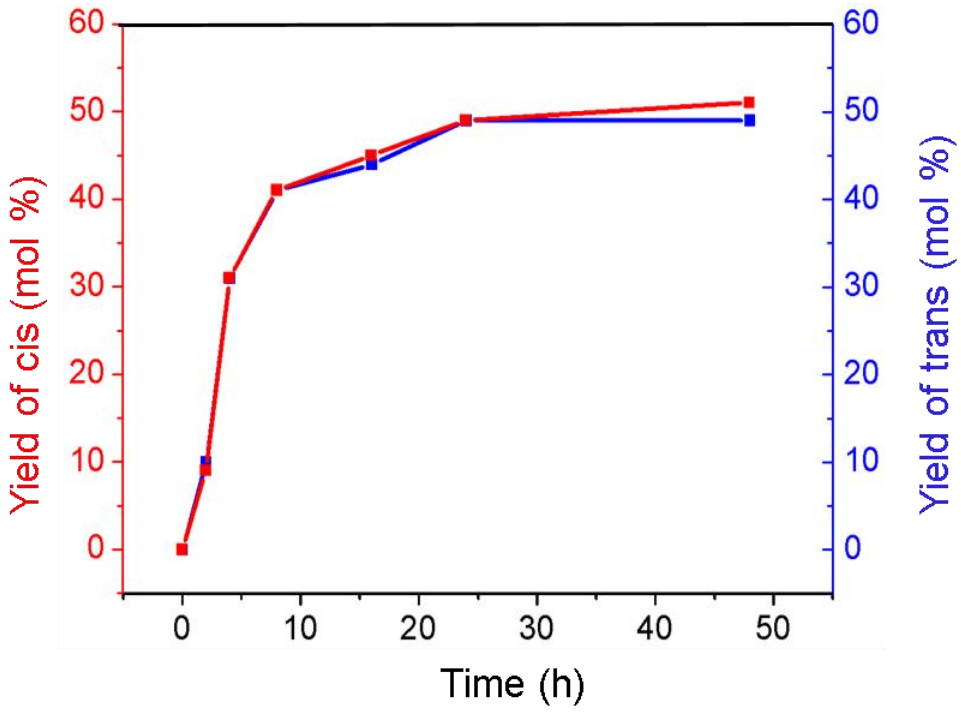

Fig. S44. Isomerization yield of *cis*-/*trans*-isomers (red / blue) in DMSO upon

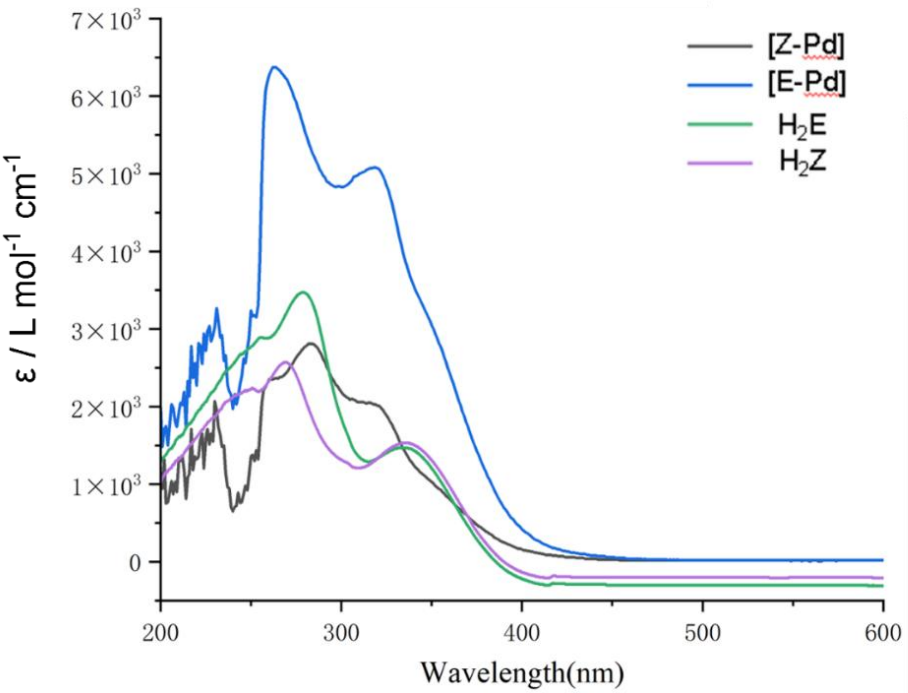

Fig. S45. UV-Vis absorption spectra of **H_2E**, **H_2Z**, **[E-Pd]** and **[Z-Pd]** in DMSO (c = 10^{-5} M).

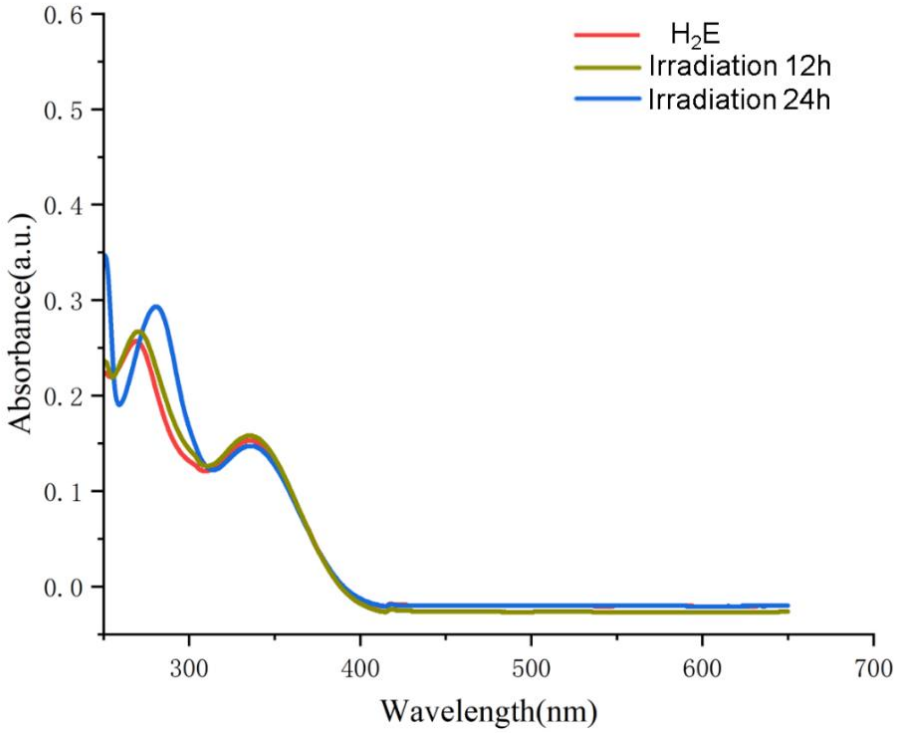

Fig. S46. Absorption spectra of **H_2E** before and after irradiation (λ = 365 nm) in DMSO (c = 10^{-5} M).

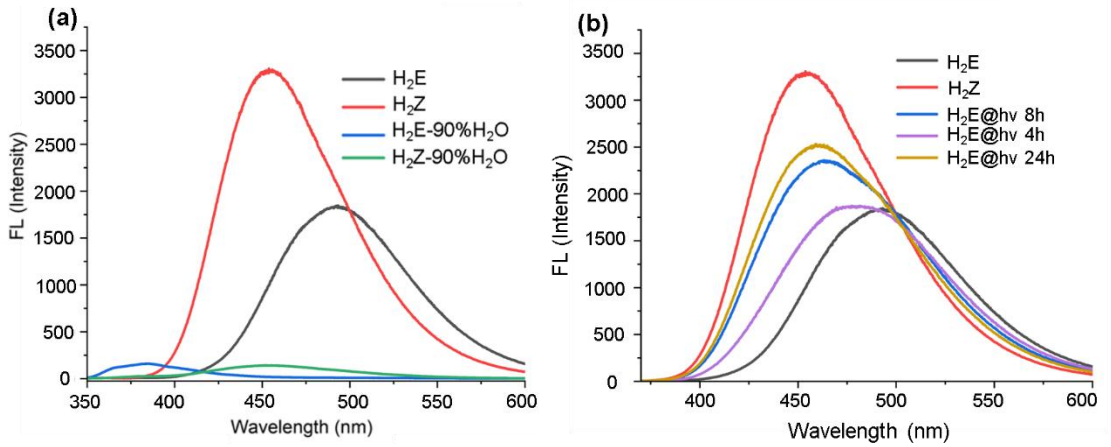

Fig. S47. Fluorescence emission spectra of **H_2E**, **H_2Z**, **[E-Pd]** and **[Z-Pd]** in DMSO and 10% DMSO-90% H_2O mixture (c = 10^{-5} M).

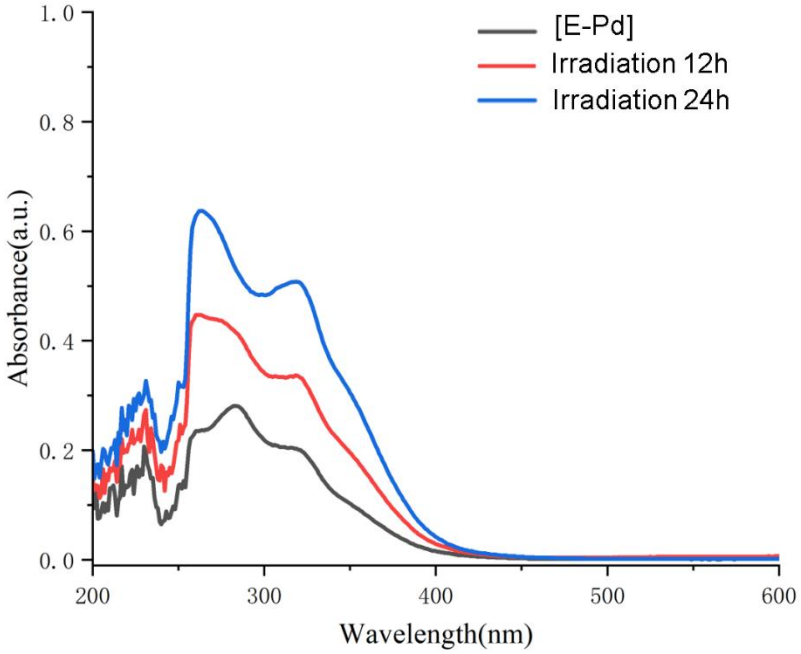

Fig. S48. Absorption spectra of **[E-Pd]** before and after irradiation (λ = 365 nm) in DMSO (c = 10^{-5} M).

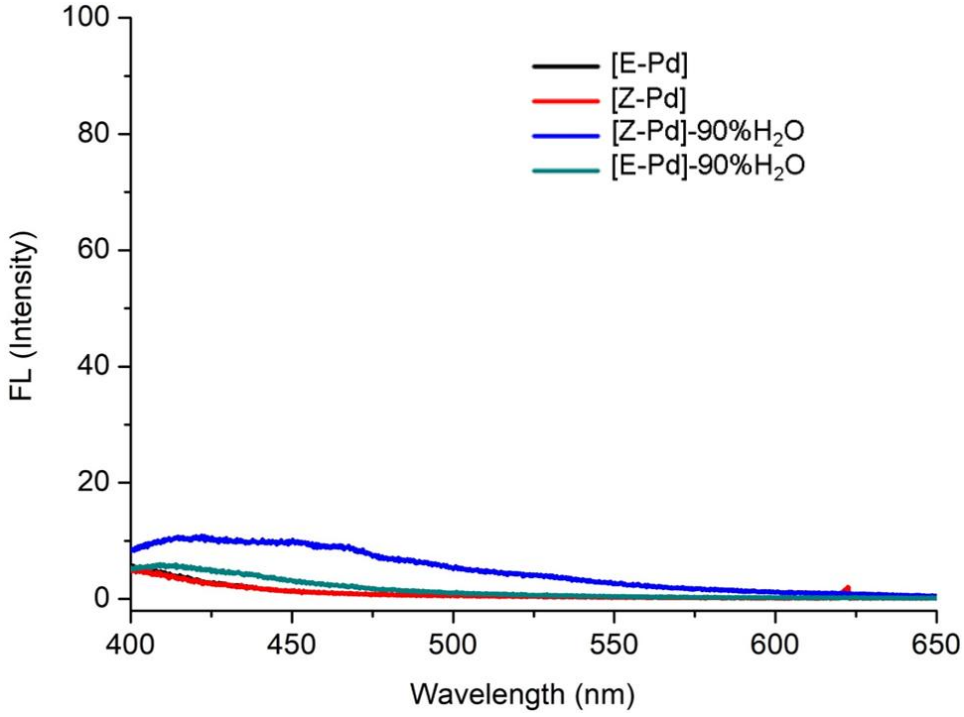

Fig. S49. Fluorescence emission spectra of **H_2E** before and after irradiation (λ = 365 nm) in 10% DMSO-90% H_2O mixture(c = 10^{-5} M)

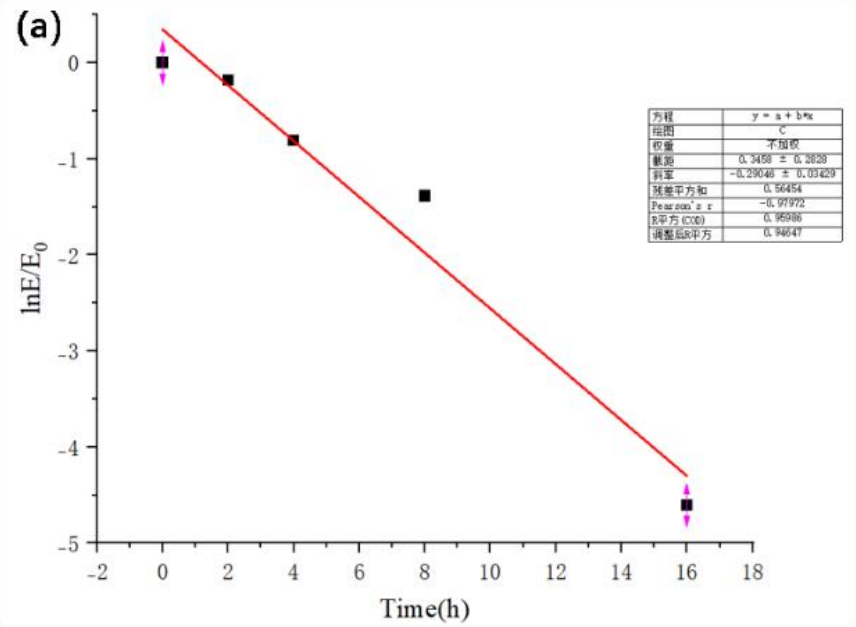

Fig. S50. Kinetic rate constants of structural transformation of [**E-Pd]** to [**Z-Pd]** under irradiation (λ = 365 nm) conditions (c = 4mM).

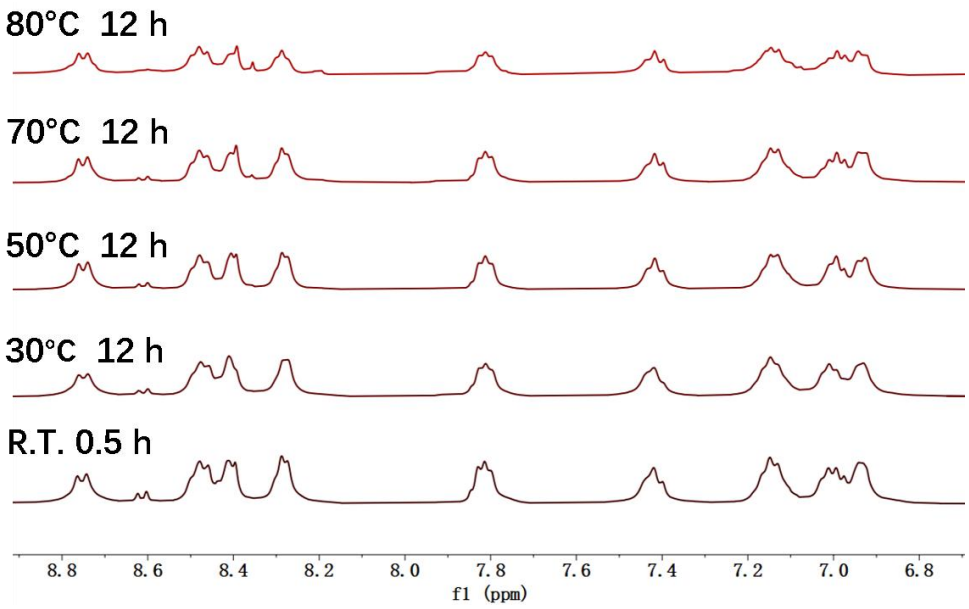

Fig. S51. ^{1}H NMR spectra of **[E-Pd]** in DMSO-d_6 after heating from room temperature to 80 °C for 48 h.

7. X-ray crystallography

A Bruker SMART APEX-II CCD X-ray diffractometer equipped with graphite monochromated Mo-Kα radiation (λ = 0.71073 Å) was used for X-Ray single-crystal structural studies of **H_2Z** and **[Z-Pt]**. The empirical absorption correction for complex was performed using SADABS[1]. The SHELXTL direct methods was used to solve all the crystal structures, which was again refined by employing full-matrix least-squares on F2 by using the SHELXTL software program and expanded using Fourier techniques.[2-3] Heavier atom Pd was determined easily, whereas, all other non-H atoms were refined with anisotropic thermal parameters, Hydrogen atoms were assigned isotropic displacement coefficients, and their coordinates were allowed to ride on their respective carbons or nitrogens. The crystal data and refinement parameters for all the crystal complexes are summarized in **Tables S2-S3**. CCDC numbers are 2157979 for **H_2Z** and 2157983 for **[Z-Pt]**.

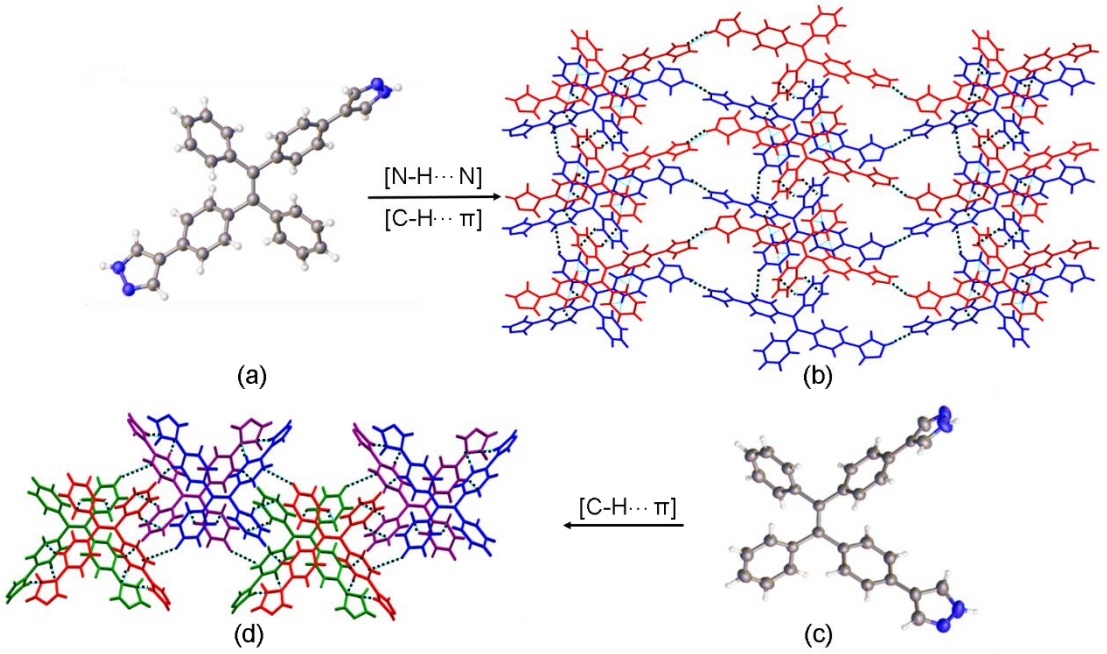

Fig. S52. Single crystal structures of ligands **H_2Z** (a), **H_2E**[4](c) and the intermolecular interactions in crystals **H_2Z** (b), **H_2E** (d).

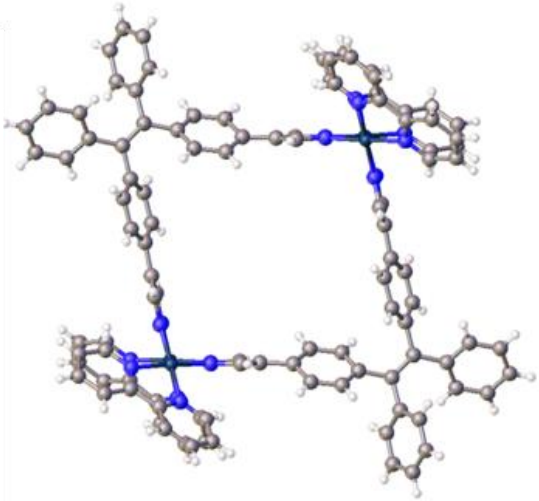

Fig. S53. Single crystal structure of **[Z-Pt]**.

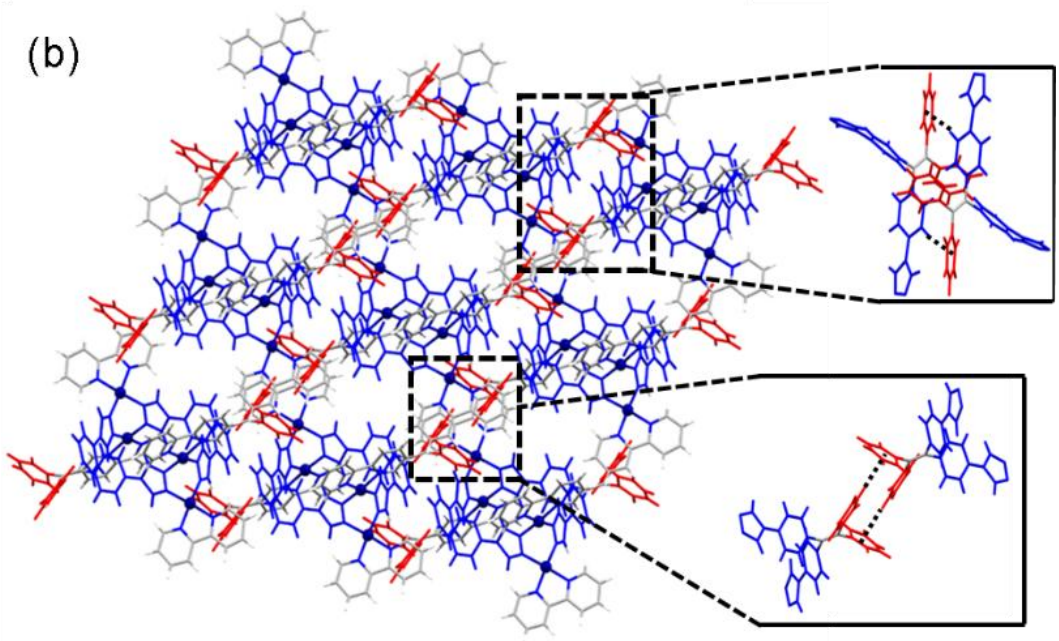

Fig. S54 The intermolecular interactions in crystal **[Z-Pt]**.

Table S2. Supermolecule Crystal and experimental data.

	Z	Z-Pt
Empirical formula	$C_{32}H_{24}N_4$	$C_{52}H_{38}N_8Pt_2$
Formula weight	464.55	1165.091
Temperature/K	193.0	173.00
Crystal system	orthorhombic	triclinic
Space group	$Cmc2_1$	P-1
a/Å	39.366(10)	13.2560(9)
b/Å	18.683(5)	13.9039(9)
c/Å	9.677(2)	19.6838(13)
α/°	90	94.852(3)
β/°	90	92.025(3)
γ/°	90	115.062(3)
Volume/Å^3	7117(3)	3264.4(4)
ρ_{calc}g/cm^3	0.867	1.185
μ/mm^{-1}	0.256	5.593
Radiation	GaKα (λ = 1.34139)	synchrotron (λ = 1.34139)
2Θ range for data collection/°	3.906 to 120.342	3.94 to 107.98
Reflections collected	54151	37438
Independent reflections	7813 [R_{int} = 0.0732, R_{sigma} = 0.0525]	11891 [R_{int} = 0.0538, R_{sigma} = 0.0499]
Goodness-of-fit on F^2	1.064	1.037
Final R indexes [I>=2σ (I)]	R_1 = 0.0653, wR_2 = 0.1900	R_1 = 0.0375, wR_2 = 0.1049
Final R indexes [all data]	R_1 = 0.1036, wR_2 = 0.2174	R_1 = 0.0463, wR_2 = 0.1092

Table S3. Selected bond lengths (Å) and bond angles (°) for **[Z-Pt]**.

Atom	Atom	Length/Å
Pt1	N1	2.012(4)
Pt1	N2	1.987(4)
Pt1	N3	1.996(4)
Pt1	$N8^1$	2.000(4)
Pt2	$N4^1$	2.003(4)
Pt2	N5	2.011(4)
Pt2	N6	2.004(5)
Pt2	N7	1.989(5)

Atom	Atom	Atom	Angle/°
N2	Pt1	N1	80.75(17)
N3	Pt1	N1	97.06(17)
N3	Pt1	N2	176.81(18)
$N8^1$	Pt1	N1	173.98(19)
$N8^1$	Pt1	N2	95.27(17)
$N8^1$	Pt1	N3	87.09(17)
N5	Pt2	$N4^1$	177.6(2)
N6	Pt2	$N4^1$	96.68(18)
N6	Pt2	N5	80.96(19)
N7	Pt2	$N4^1$	86.07(18)
N7	Pt2	N5	96.27(19)
N7	Pt2	N6	176.99(16)

References

1. Crystal reference: SAINT, Program for Data Extraction and Reduction, Bruker AXS, Inc., Madison, WI, 2001.

2. G. M. Sheldrick, SADABS, Program for Empirical Adsorption Correction of Area Detector Data, University of Göttingen, Göttingen, Germany, 2003.

3. G. M. Sheldrick, SHELXS-2014, Program for the Crystal Structure Solution, University of Göttingen, Göttingen, Germany, 2014.

4. Wen, J.; Tong, J.; Kou, Y-L.; Wang, J.; Yu, S-Y. Multi-responsive smart fluorophores from pyrazole-functionalized tetraphenylethene AIEgens in response to Hg(II) ion, temperature, and mechanical force. Dyes Pigments, 2024, 223, 11195.